New Approaches to Lunar Ice Detection and Mapping

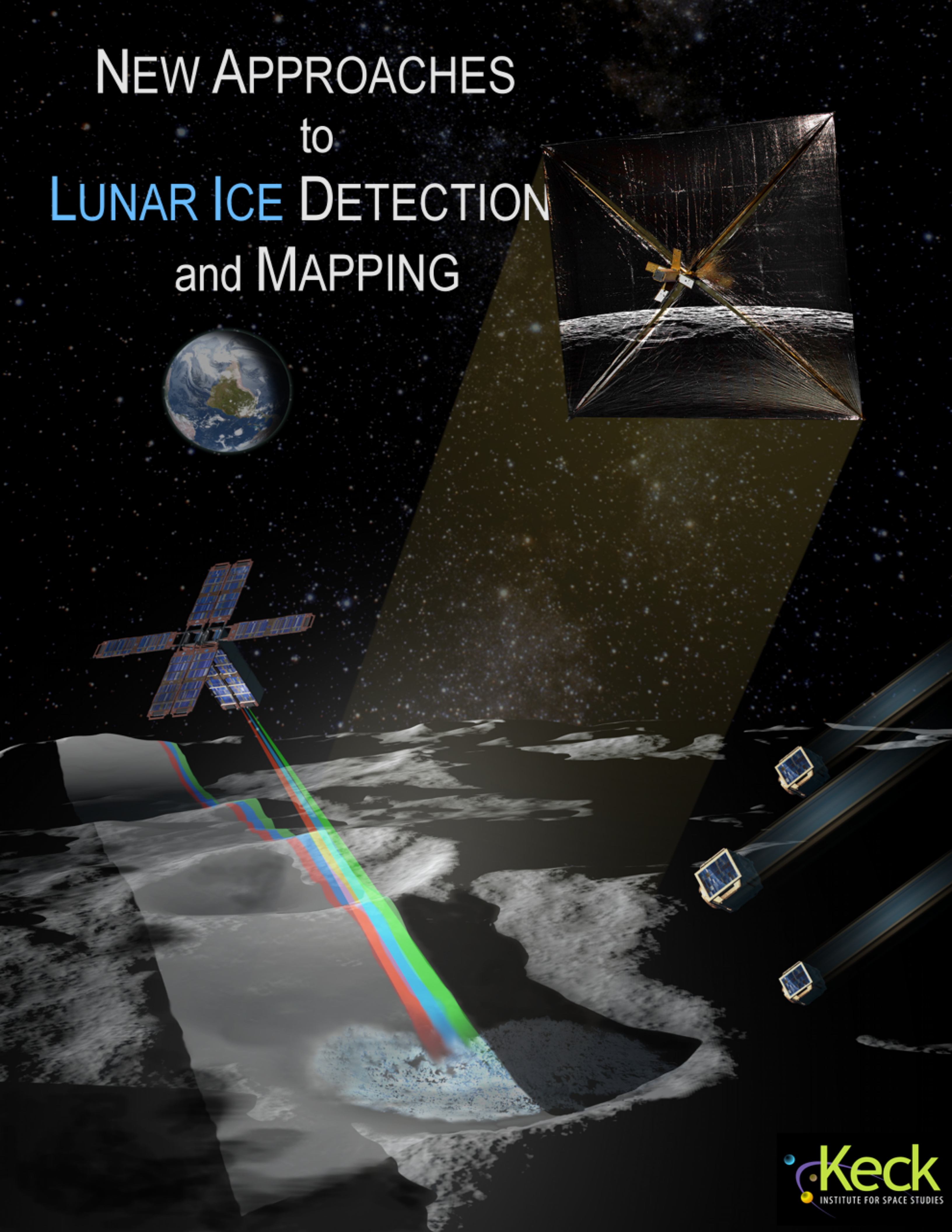

Keck Institute for Space Studies

New Approaches to Lunar Ice Detection and Mapping

Study start date: July 22, 2013
Study end date: November 7, 2013
Final Report submission date: April 30, 2014

Study Leads:

Paul O. Hayne
Jet Propulsion Laboratory
California Institute of Technology
Paul.O.Hayne@jpl.nasa.gov

Andrew P. Ingersoll
Division of Geological & Planetary Sciences
California Institute of Technology
api@gps.caltech.edu

David A. Paige
Department of Earth, Planetary & Space Sciences
University of California, Los Angeles
dap@mars.ucla.edu

Study Participants

Oded Aharonson	Weizmann Institute of Science
Leon Alkalai	Jet Propulsion Laboratory, California Institute of Technology
Shane Byrne	University of Arizona
Yang Chen	Jet Propulsion Laboratory, California Institute of Technology
Barbara Cohen	NASA – Marshall Space Flight Center
Anthony Colaprete	NASA – Ames Research Center
Jean-Philippe Combe	Bear Fight Institute
Christopher Edwards	California Institute of Technology
Bethany Ehlmann	California Institute of Technology
William Feldman*	Planetary Science Institute
Emily Foote	University of California, Los Angeles
Benjamin T. Greenhagen	Jet Propulsion Laboratory, California Institute of Technology
Paul O. Hayne (Co-Lead)	Jet Propulsion Laboratory, California Institute of Technology
Amanda Hendrix	Planetary Science Institute
Brendan Hermalyn	University of Hawaii
Andrew P. Ingersoll (Co-Lead)	California Institute of Technology
Yang Liu	Jet Propulsion Laboratory, California Institute of Technology
Paul G. Lucey	University of Hawaii
Benjamin Malphrus	Morehead State University
Timothy P. McClanahan	NASA – Goddard Space Flight Center
Daniel J. McCleese	Jet Propulsion Laboratory, California Institute of Technology
Thomas B. McCord	Bear Fight Center
Catherine Neish	Florida Institute of Technology
Gregory Neumann	NASA – Goddard Space Flight Center
Raquel Nuno	Arizona State University
David A. Paige (Co-Lead)	University of California, Los Angeles
Cedric Pilorget	California Institute of Technology
Michael Poston	Georgia Institute of Technology
Gerald Sanders	NASA – Johnson Space Center
Norbert Schorghofer	University of Hawaii
R. Glenn Sellar	Jet Propulsion Laboratory, California Institute of Technology
Matthew Siegler	Jet Propulsion Laboratory, California Institute of Technology
Robert Staehle	Jet Propulsion Laboratory, California Institute of Technology

*Distinguished Visiting Scientist

Acknowledgments

The research described in this report was sponsored by the Keck Institute for Space Studies (KISS) and was carried out in part at the Jet Propulsion Laboratory, California Institute of Technology, under a contract with the National Aeronautics and Space Administration. We thank Martin Lo for contributions related to the navigation of small satellites for lunar science. Conversations with numerous non-study participants, including Dana Hurley, David Lawrence, Wesley Patterson, and Ben Bussey, were extremely helpful. The success of this study would not have been possible without technical guidance and logistical support from the KISS staff, particularly Michele Judd.

Table of Contents

Acronyms and Abbreviations

ACS	Attitude control system
AVGR	Ames Vertical Gun Range
CHACE	Chandra's Altitudinal Composition Explorer
COTS	Commercial, off-the-shelf
COVE	CubeSat Onboard processing Validation Experiment
CPR	Circular polarization ratio
CXBN	Cosmic X-ray Background Nanosatellite
DAN	Dynamic Albedo of Neutrons experiment
DI	Deep Impact
ESPA	Evolved Expendable Launch Vehicle Secondary Payload Adapter
GC	Gas chromatography
GCMS	Gas chromatography/mass spectrometry
GCR	Galactic cosmic rays
GSFC	Goddard Space Flight Center
INSPIRE	Interplanetary NanoSpacecraft Pathfinder In a Relevant Environment
IPEX	Intelligent Payload Experiment
IPH	Interplanetary hydrogen
IR	Infrared
ISARA	Integrated Solar Array and Reflectarray Antenna
ISRU	In Situ Resource Utilization
JPL	Jet Propulsion Laboratory
KISS	Keck Institute of Space Studies
LADEE	Lunar Atmosphere and Dust Environment Explorer
LAMP	Lyman-α Mapping Project
LCROSS	Lunar CRater Observation and Sensing Satellite
LEND	Lunar Exploration Neutron Detector
LEO	Low Earth Orbit (160 – 2,000 km)
LET	Linear energy transfer
LIDAR	Laser ranging system
LOLA	Lunar Orbiter Laser Altimeter
LP	Lunar Prospector mission
LRO	Lunar Reconnaissance Orbiter mission
LT	Lunar Trailblazer proposed mission concept
M^3	Moon Mineralogy Mapper
MEMS	Microelectromechanical systems
MESSENGER	MErcury Surface, Space ENvironment, GEochemistry and Ranging mission
MIRO	Microwave Instrument for the Rosetta Orbiter
MSL	Mars Science Laboratory
NS	Neutron spectrometer

O/OREOS	Organism/Organic Exposure to Orbital Stresses
ORS	Operationally Responsive Space Office (NASA)
OCT	NASA Office of the Chief Technologist (now: STMD)
PSR	Permanently shadowed region
QMS	Quadrupole mass spectrometer
SEE	Single event effect
STMD	NASA Space Technology Mission Directorate
TID	Total integrated dose
TLS	Tunable laser spectrometer
WMB	Watson, Murray, and Brown (1961)

1 Executive Summary

As a fundamental molecule to life on Earth, water is a key marker of habitable environments in the Solar System. Yet after decades of exploration, the origins, abundance, and distribution of water amongst the planets are not fully understood. The recent discovery of substantial water ice deposits in the polar regions of both Mercury and the Moon presents an opportunity to test hypotheses regarding the delivery and retention of water and other volatiles in the inner Solar System. As the Earth's closest planetary neighbor, the Moon thus may be a uniquely accessible keystone for addressing outstanding problems in planetary science directly linked to habitability. Furthermore, water on the Moon is of great interest to the exploration community, as a resource for astronauts and robotic missions of the future.

The first major goal of this study was to identify the outstanding questions about lunar volatiles that could be addressed by new observations. In order to define the key measurements, we identified two fundamental questions driving the science and exploration of lunar volatiles:

1. *What are the origins and evolution of water in the inner Solar System?*
2. *Where are the operationally useful deposits of water on the Moon?*

Existing data have only scratched the surface with regard to the abundance and distribution of water on the Moon, let alone its origins. Spacecraft remote sensing data suggest enhanced hydrogen in both polar regions [*Feldman et al*., 1998] and nearly ubiquitous water of hydration in the lunar regolith [*Pieters et al*., 2009; *Clark*, 2009; *Sunshine et al.,* 2009], yet its form and abundance are poorly constrained [*McCord et al*., 2011]. Water and other comet-like volatiles excavated from the LCROSS impact site near the lunar south pole suggest concentrations of H_2O could be locally present in quantities useful for *in situ* science and resource utilization [*Colaprete et al*., 2010]. However, remote sensing data provide ambiguous, and often conflicting information about the abundance and distribution of volatiles at the lunar poles [*Mitrofanov et al*., 2010; *Paige et al*., 2010]. Determining whether and what types of new data could solve the debate was a primary goal of this study. As detailed in this report, we identified several measurement approaches with a high likelihood of satisfying the following key requirement:

Determine the concentration of water in the upper few meters of lunar regolith with sensitivity better than 0.5wt%, at multiple locations with diverse thermal environments

Combined with existing datasets, these new measurements will address the origins and distribution of water in the Earth-Moon system, and will enable informed landing site selection for future missions. The study prioritizes several specific measurement techniques falling under each of the following mission types:

- **Orbiting spacecraft**: *active* multispectral reflectance measurements in the ultraviolet to near-infrared spectral range and/or *passive* multispectral emission measurements in the thermal infrared, for definitive detection and mapping of water and other volatiles within several micrometers of the surface
- **Impactor probes**: targeted, well characterized impacts to kinetically excavate the subsurface, observed from a separate Moon- or Earth-based platform in the ultraviolet to microwave spectral range to detect ice and vapor released at several distinct sites
- **Penetrator probes**: targeted, instrumented probes capable of detecting ices and quantifying their depth distribution at several distinct sites using neutron spectroscopy, mass spectroscopy, and/or tunable laser spectroscopy
- **Landers and rovers**: instrumented platforms with a drill or excavator, capable of measuring the composition and abundance of ices at the surface and subsurface within a relatively confined region of the Moon

Potential science return from each of these approaches is high, although there is a significant tradeoff between spatial (i.e., lateral) and depth coverage among them. Although the study did not explicitly consider cost, we carefully assessed the likelihood that small, low-cost spacecraft could be used to accomplish each of these approaches. The current state of the art for landers, rovers, and some orbital measurements falls outside of this category; thus, they were not studied in detail. Penetrator probes are relatively small and inexpensive, but have large uncertainties in both cost and technical readiness for this application [*Lorenz*, 2011]. Small satellites were found to be particularly well suited to the envisioned orbiter and impactor mission designs, and were therefore studied in the greatest detail.

The second major goal for this study was to seek ways to harness emerging small spacecraft technologies for low-cost lunar missions. Since their advent in the 1990's, nanosatellites (and the CubeSat form factor in particular) have rapidly evolved and are now routinely built (primarily by university students) and launched to low-Earth orbit (LEO) for science, technology, and education applications. With their rapid development times and extremely low cost compared to traditional spacecraft, nanosatellites and other small satellites present an exciting new paradigm to planetary science, if their capabilities can be proven beyond low Earth orbit. The Moon is ideally situated for the first of these missions. We therefore assessed whether or not one or more small satellite missions could accomplish the desired lunar ice detection measurements.

In this report, we propose a new program of lunar science and exploration by small, low-cost spacecraft. Initially, this program will be guided by the above measurement goals relevant to detection and mapping of lunar volatiles, but could later be expanded to other investigations of the Moon and beyond. As a first step, we advocate sending a "trailblazer" nanosatellite to a polar lunar orbit, which would carry a limited yet useful payload (see Section 5). The goal of this mission would be to prove that scientifically valuable data on lunar volatiles could be acquired using a nanosatellite at a total cost of <$10M. Some of the key technologies needing development are identified in this report. Following the pathfinder mission, one or more additional small satellites would carry instrumentation specifically designed for the measurements outlined above. Ultimately, we envision a fleet of tiny spacecraft, each with its own specialized yet synergistic payload for detecting, mapping, and characterizing lunar ice deposits. If successful, such a program has the potential to accomplish as much as a traditional spacecraft mission, at a fraction of the cost. Finally, this program could pave the way for more ambitious spacecraft missions beyond the Moon, thereby opening up a new paradigm in planetary exploration.

2 Introduction

Recent spacecraft investigations have provided tantalizing yet often conflicting evidence for water ice and other volatile species at the Moon's poles. Substantial deposits of ices (H_2O, NH_3, CO_2, H_2S, etc.) may be hidden within perennial shadows where temperatures are among the coldest in the Solar System [*Paige et al.*, 2010]. Such polar ice reservoirs have been predicted for nearly a century based on theoretical models [*Goddard*, 1920; *Watson et al.*, 1961a] and could represent a relatively pristine and scientifically valuable record of volatile delivery to the Earth-Moon system. If sufficiently accessible, near-surface ice deposits could also provide resources (propellants, water, oxygen) for use by robotic and human explorers.

However, fundamental uncertainties about the abundances and distribution of lunar ices must be addressed before robots or humans can locate and extract them. Recent narrow-band reflectivity data from the Lunar Reconnaissance Orbiter (LRO) suggest volatiles may be present on the surface, yet surface roughness effects cannot be ruled out [*Zuber et al.*, 2012; *Gladstone et al.*, 2012]. Radar data are ambiguous [*Spudis et al.*, 2010, 2013], and hydrogen mapped by neutron spectroscopy does not clearly correlate with cold regions observed in the thermal infrared [*Sanin et al.*, 2012]. The LCROSS mission [*Colaprete et al.*, 2010] detected water and other volatiles in potentially useful abundances (~5 wt% H_2O) for the first time, but at a single location. As we reach the limits of existing data, it is clear that a new type of mission is needed to investigate and map these important inner solar system ice reservoirs.

The primary objective of this study was to explore innovative, low-cost mission concepts for detecting and mapping "operationally useful" ice deposits on the Moon, defined as those accessible to surface landers or rovers. In the following sections, we first summarize results from previous missions and current understanding of this topic (Section 2.1). Section 2.2 describes recent advancements in small, low-cost spacecraft technology that provided additional motivation for initiating this study. In Section 3 we outline the study format. The results of the study are detailed in Section 4, which provide the basis for the proposed future directions in Section 5.

2.1 Scientific Background

Water may be stored in cold permanently shadowed regions (PSRs) near the lunar poles and transported there from an exogenic or endogenic source via ballistic hops of H_2O molecules, sustained against several loss processes (Fig. 1). This theoretical concept, known as the "WMB" mechanism (after *Watson, Murray, and Brown*, [1961a,b]), remains unproven, but several missions over the past two decades (e.g., LRO, Lunar Prospector, etc.) have revealed evidence for water on the Moon. Reviews on this topic are available by *Arnold* [1979], *Lucey* [2009a], and *Basilevsky et al.* [2012]. Here we briefly summarize the scientific understanding and observational constraints with an emphasis on recent results. Results from the LADEE mission were not yet available as of this writing, and thus not incorporated in this review. Section (2.1.1) reviews theoretical developments, section (2.1.2) succinctly lists available observational constraints, and section (2.1.3) reviews the case of Mercury, which represents the best evidence for cold trapping of water ice.

2.1.1 Theory

There are three equally important components to the delivery and trapping process for lunar volatiles: their source(s), transport to the polar regions, and ultimate storage.

Sources/Origin:
Numerous exogenic and endogenic sources have been proposed as the source of lunar volatiles (comets, interplanetary dust particles, meteorites, production on the surface via solar wind, and others) and are reviewed in *Arnold* [1979]. Among the recent results that may be relevant to this question is the production of H_2O from recombination of OH at high temperature (~400K), with subsequent transport of water molecules to the polar regions [*Dyar et al.*, 2010; *Poston et al*., 2013]. One major outstanding question is the age of any ice reservoir, i.e., whether it is geologically recent or primordial. The isotopic composition of any lunar ice would provide insight into the origin of the ice, although the fractionation that occurs during the transport to the cold traps is uncertain.

Transport:
Lateral transport is essential for delivering water from any other part of the Moon into the cold traps. The following alternatives can be considered:

a) A transient atmosphere after impact of a large comet would liberate significant H_2O
b) Efficient lateral transport by ballistic hops (Fig. 1)
c) No or inefficient lateral transport

The classic WMB theory relies on migration of water molecules by ballistic hops. The feasibility of this process has been questioned by *Hodges* [2002], who argues that H_2O will be chemisorbed upon contact with an extremely dry and space weathered lunar grain. This argument was in part based on the behavior of argon, though recent measurements have been less clear on the presence of Ar in the lunar exosphere [*Cook et al.*, 2013, 2014]. Nevertheless, uncertainties remain about the interaction of H_2O and OH with silicate grains on the lunar surface.

Shortwave-infrared spectroscopy has revealed an OH/H_2O absorption band at high latitudes (>60° on both hemispheres) on the Moon, and, in one case, at both lunar terminators [*Clark*, 2009; *Pieters et al.*, 2009; *Sunshine et al.*, 2009], though it is difficult to distinguish between OH and H_2O using these measurements. Enhanced absorption at the terminators would imply diurnal variation of the surface concentration. However, temperature dependent thermal emission complicates the interpretation of the absorption band [*Lucey*, 2009b]. Theoretically, migrating water is expected to enhance concentrations at only one terminator [*Schorghofer*, 2012]. Independent of these results, the mass spectrometer on the Chandra's Altitudinal

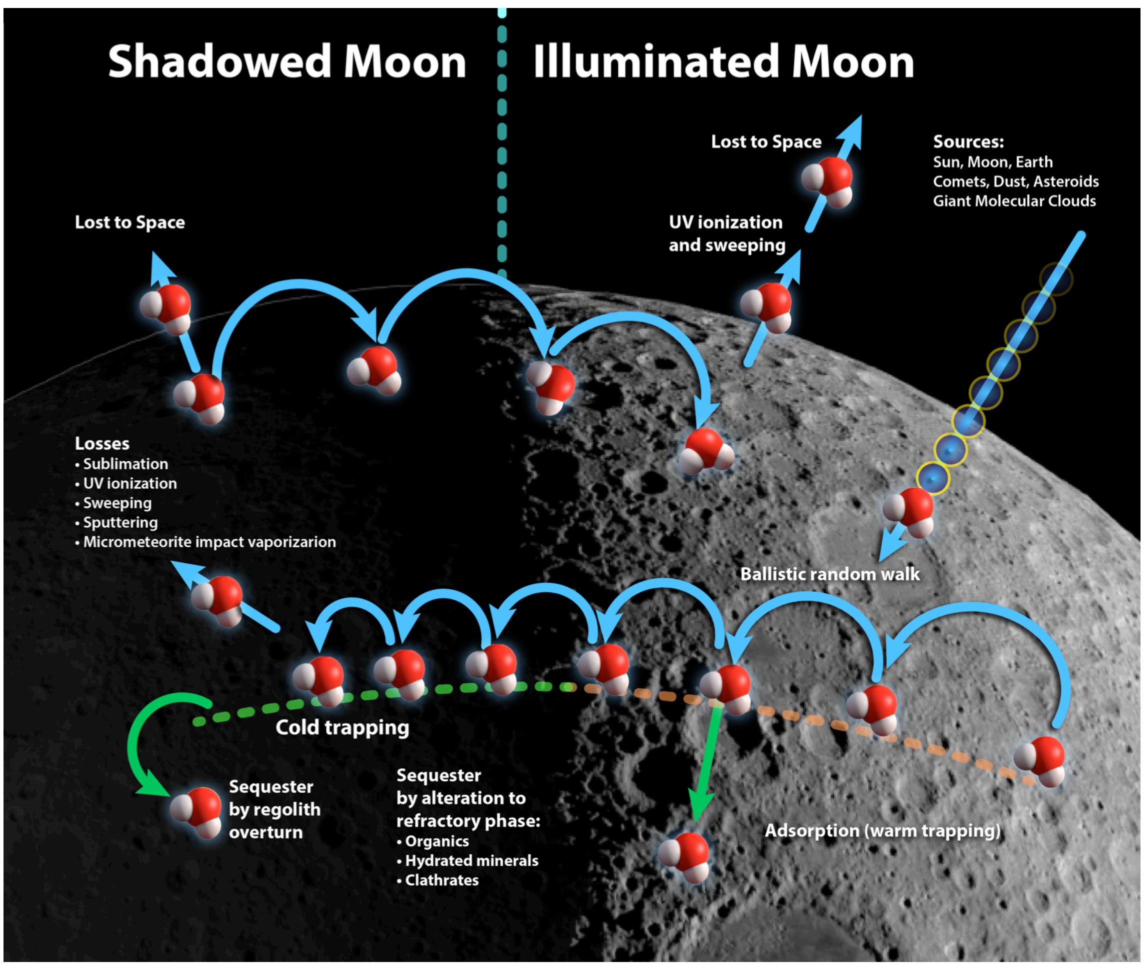

Figure 1: Processes involving volatiles in the polar regions of the Moon.

Composition Explorer (CHACE) instrument on Chandrayaan-1 has detected H_2O in the exosphere [*Sridharan et al*., 2010], while previous measurements have detected several species, but no H_2O [*Stern*, 1999; *Cook et al*., 2013]. Whether any migration of H_2O or OH presently occurs or has occurred on the Moon remain open questions.

Storage:

a) At low temperature the sublimation rate of ice becomes negligible (<1m/Ga for <120K). Among common volatiles, H_2O has the lowest vapor pressure. *Zhang and Paige* [2009] have compiled sublimation rates for organics, hydrocarbons, etc. The classic theory (WMB) envisioned exposed ice in large cold craters (cf. *Vasavada et al*., [1999]). Two variants of the classic storage geometry have been proposed: 1) the ice may be buried, and thus last at somewhat higher temperatures [*Schorghofer,* 2008; *Paige et al.*, 2010], and 2) small shadows from large boulders and small craters near the poles may also act as cold traps resulting in a patchy distribution of ice with the resulting cumulative area being of comparable size to that of the large cold traps [*Hayne et al.*, 2013a].

b) Adsorption [*Cocks et al.*, 2002] or hydration: H_2O might not be in crystalline or amorphous form, but individual H_2O molecules may be adsorbed on grain surfaces. However, this storage mechanism would require very high specific surface area to produce the abundances measured by neutron spectroscopy. Alternatively, hydrogen could be incorporated in the crystal lattice structure, but abundant hydrated minerals are not observed on the lunar surface [*Pieters et al.*, 2009].

c) Diffusion-limited escape of implanted solar wind ions [*Starukhina*, 2001, 2006; *Boynton et al*., 2012): this theory proposes that solar wind protons are implanted in the regolith where at high temperature these quickly escape, but at low temperature their escape is thermally inhibited and protons accumulate to saturation. Since the temperature dependence is strong (Boltzmann factor), an abrupt geographic boundary can be expected. In this case the measured hydrogen is not carried in the form of H_2O, but rather as protons bonded to oxygen atoms in lunar minerals. This concept was originally proposed for the PSRs but has also been considered as possible explanation for the OH-band observed spectroscopically at polar latitudes [*Clark*, 2009].

d) The ice pump mechanism [*Schorghofer and Aharonson*, 2014] does not exhibit a simple temperature dependence. Under suitable conditions, H_2O molecules can be “pumped down” into the regolith by day-night temperature cycles. The amplitude of surface temperature oscillations quickly decays with depth, and the strongly nonlinear dependence of molecular residence times on temperature leads to vertical drift processes. Volatile H_2O molecules on the surface are needed as a source for the pump.

It remains unclear whether water ice in the PSRs could be exposed on the surface or only buried beneath the surface. If buried, it may have a layered structure, might be mixed with regolith by impact gardening, or distributed as impact ejecta. Some type of inhomogeneity can be expected in all cases.

2.1.2 Observations

Water or hydroxyl has been detected at the lunar surface by passive infrared spectroscopy using measurements from three spacecraft (Cassini, Deep Impact and Chandrayaan-1 [*Clark*, 2009; *Pieters et al*., 2009; *Sunshine et al*., 2009]) that showed strong absorption in the 3-μm region. Water (or at least hydroxyl) was long anticipated owing to interaction of solar wind protons and lunar surface oxygen [*Zeller et al*., 1967], but until the three spacecraft measurements this possibility remained a hypothesis.

The 3-μm measurements also feature strong variations in the intensity of the hydroxyl/water band with lunar time of day, with significant implications for lunar science. If the abundance of water is variable, this may imply that the water is mobile and migrating to cooler portions of the lunar surface. However, the lifetime of the water molecule against ionization and sweeping is only about 20 hours, so mobile water would not be recycled and requires a constant flux of new water [*Potter and del Duca*, 1964; *Allen et al*., 1987; *Morgan and Shemansky*, 1991; *Cochran and Schleicher*, 1993]. A portion of this constant flux would trap at the poles prior to sweeping, providing a substantial source for polar water. *Hendrix et al*. [2012] showed that two color ultraviolet data from the LRO LAMP experiment varied with lunar time of day, and that this was consistent with variation in water at the lunar surface, and this water could supply the poles. Remote sensing of intrinsic water that does not vary does appear to occur in some lunar locations that are likely to be associated with "wet" (~100 ppm) samples [*Klima et al*., 2013].

Additional observations over the last few decades have painted an intriguing patchwork picture of water and other volatiles on the Moon:

- Earth-based radar shows no evidence of water ice on the Moon [*Stacy et al*., 1997], although the same type of measurement revealed significant evidence for water ice on Mercury [*Slade et al*., 1992].

- The Clementine bistatic radar experiment provided tantalizing hints for water ice on the lunar south pole [*Nozette et al*., 1996].

- The Lunar Prospector Neutron Spectrometer found evidence for H-enrichment in both polar regions of the Moon [*Feldman et al*., 1998, 2000, 2001].

- The Moon Mineralogy Mapper, Deep Impact, and VIMS visible/shortwave infrared spectrometers detected spatially variable 3-μm absorptions related to

OH/H_2O, confirming a hydroxylated/hydrated component on the lunar surface [*Pieters et al*., 2009; *Sunshine et al*., 2009; *Clark*, 2009].

- LCROSS: The most direct evidence for concentrated H_2O (rather than just H) comes from the LCROSS impact, whose impact plume contained 5.6+/-2.9% of H_2O [*Colaprete et al*., 2010]. The lower end of this range may just barely qualify as a 'macroscopic' concentration, while the upper end represents nearly pore-filling ground ice.

- LOLA reflectivity measurements hint at a high albedo surface inside Shackleton Crater that could be due to exposed ice [*Zuber et al*., 2012].

- Mini-RF (radar) observations indicate a patchy, heterogeneous enhancement in CPR (circular polarization ratio). The same CPR pattern is consistent with wavelength-scale surface roughness, but some polar craters exhibit high CPR only in their interiors, consistent with the presence of water ice [*Thomson et al*., 2012; *Spudis et al*., 2013].

- LEND has provided (uncollimated) neutron counts consistent with the Lunar Prospector results. Its collimated results show enhanced H in only a few of the coldtraps [*Mitrofanov et al*., 2010, 2012; *Boynton et al*., 2012]. Diurnal variations in neutron counts at lower latitudes may also be consistent with daily water fluxes into and out of the regolith [*Livengood et al*., 2014].

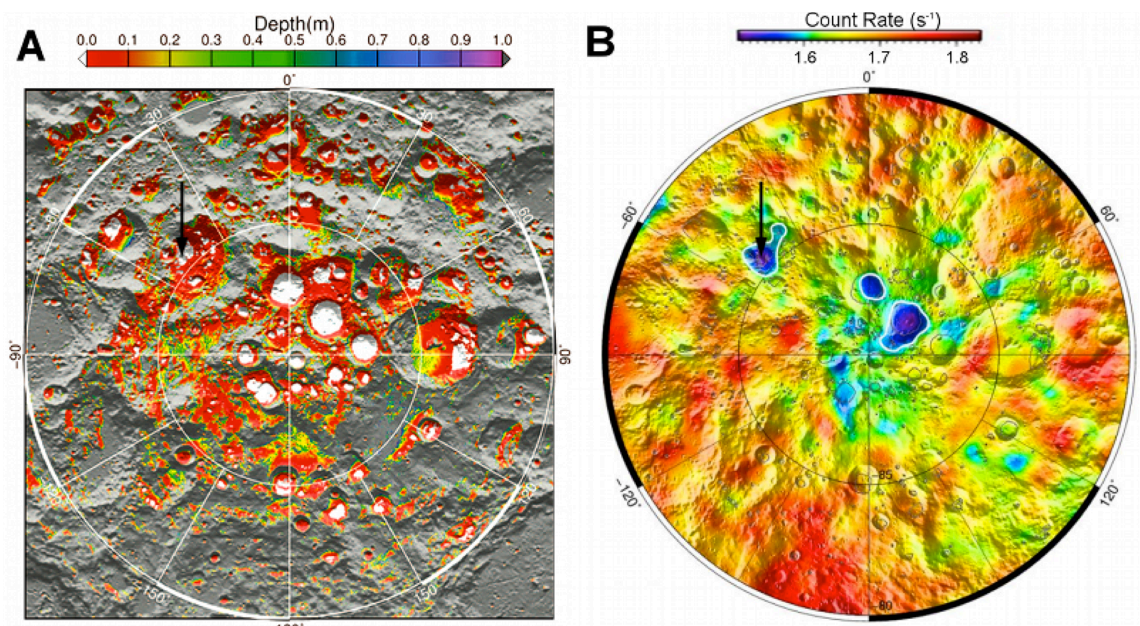

Figure 2: Example remote sensing data for the lunar south polar region. (A) Depth to water ice thermal stability (stable > 1 Gyr), based on data from Diviner [Paige et al., 2010]; (B) Epithermal neutron count rates from LEND, where lower count rates indicate enhanced H abundance [Sanin et al., 2014]. The arrow indicates the LCROSS impact site. While several of the coldest regions also show enhanced hydrogen, many do not, and vice versa.

- LAMP: Reflected Lyman-alpha sky-glow and starlight produce a UV signal from within the Moon's permanently shadowed regions. These are consistent with the presence of a small amount of frost and even with diurnal variations in hydration at low latitudes [*Gladstone et al*., 2012; *Hendrix et al*., 2012].

In summary, there is considerable observational evidence for water in both polar regions of the Moon, but the geographic distribution of H_2O is poorly constrained; observations have produced conflicting evidence (Fig. 2). Even the mere presence of widespread concentrated water ice has yet to be established, outside of the LCROSS impact site (Fig. 3). These factors make site selection for landers and rovers difficult.

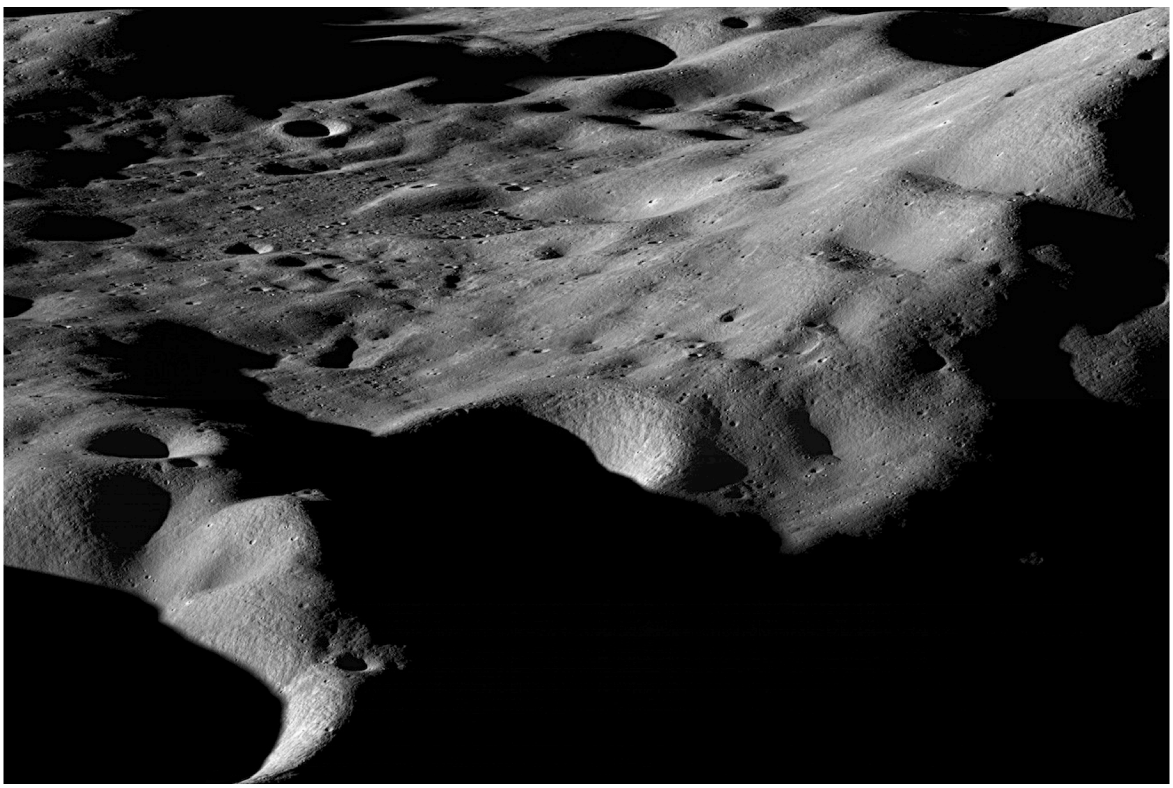

Figure 3: Oblique view of the northern rim of Cabeus crater as imaged by the Lunar Reconnaissance Orbiter Camera (LROC), from ~50 km above the surface. The LCROSS probe impacted within the permanent shadow near the bottom-middle of the frame. Many of the shadowed regions in this image are PSRs. (Credit: Arizona State U./NASA)

Table 1: Summary of observations relevant to lunar water detection and mapping

Technique	Result	Sensitivity	Depth	Resolution	Reference
Earth-based radar	Non-detection	>10-cm ice blocks	~1 m	125 m	*Stacy et al.* [1997]
Orbital mono-static radar	Disputed detection	>10-cm ice blocks	~1 m	75 m	*Spudis et al.* [2013]
Orbital bi-static radar	Disputed detection (Clementine); improved data pending (LRO)	>10-cm ice blocks	~1 m	75 m	*Patterson et al.* [2014]
Neutron spectroscopy	Detection of [H] = 1700 ± 900 ppm (~1% H_2O) average >70° latitude	H atoms at greater than ~100 ppm	~1 m	~50 km	*Feldman et al.* [2000, 2001]
Neutron spectroscopy	Detection of [H]; specific PSRs with ~200 – 4500 ppm (0.1% - 4% H_2O)	H atoms greater than ~100 ppm	~1 m	~10-50 km	*Mitrofanov et al.* [2012]
Infrared spectroscopy of impact plume	Detection of 5.6 ± 2.9% H_2O, at single point (84.7°S, 310.6°E)	H_2O ice and vapor at greater than ~1wt%	~3 m	30-m crater	*Colaprete et al.* [2010]
Ultraviolet spectroscopy	Possible detection in the PSRs; detection of H_2O (and diurnal variations) at low latitudes	H_2O with abundance greater than ~0.5wt%	~1 µm	240 m	*Gladstone et al.* [2012], *Hendrix et al.* [2012]
Infrared solar reflectance spectroscopy	Detection of 10 – 100 ppm OH and H_2O on mineral surfaces under direct solar illumination	H_2O and OH with abundance greater than ~10 ppm	~10 µm	140 m	*McCord et al.* [2011]
Analysis of lunar samples	Detection of ~0 – 1wt% H_2O in igneous melt inclusions	Various	Surface	-	*Boyce et al.* [2010], *Liu et al.* [2012]

2.1.3 Comparisons with Mercury

Motivation for searching for water cold-trapped in permanently shadowed craters on the Moon is also provided by Mercury, where radar, neutron spectroscopy, and laser reflectivity all provide compelling evidence for the presence of ice. Furthermore, there appears to be a one-to-one correspondence between cold traps and ice deposits [*Chabot et al*., 2013]. Earth-based radar has long suggested the presence of thick massive ice deposits on Mercury [*Slade et al*., 1992]. Neutron spectroscopy of the north polar region by the MESSENGER spacecraft shows a significant enhancement of hydrogen [*Lawrence et al*., 2013]. Laser albedo measurements along laser altimeter tracks indicate high albedo material is coincident with the very coldest locations, plausibly representing exposed ice [*Neumann et al*., 2013]. In adjacent slightly warmer but still cold-trapping areas, the albedo is especially low and may indicate a dark sublimation lag of less volatile materials [*Paige et al*., 2013]. It has been argued that the burial rate, due to impact ejecta, is fast enough that any exposed ice must be recent, on the order of 50Myr [*Crider and Killen*, 2005].

Current evidence indicates the Moon has much less water ice than Mercury, though the reason for this difference in volatile abundances remains a major open question. One possibility is orbital-rotational dynamics: the Moon underwent a major spin axis excursion a few billion years ago [*Ward*, 1975], which must have temporarily erased all permanently shadowed areas, while Mercury's spin axis has remained locked since soon after its formation. Alternatively, the supply of water to Mercury's surface may be higher than that of the Moon. Mercury's interior structure is very different from that of the Moon, and may have experienced significantly more outgassing than the Moon. If the main source of water comes from solar wind interactions, Mercury's proximity to the sun could also be an important factor. If the main source of water is comets, a large population of sun-grazers may deliver more water to Mercury than to the Moon.

2.2 Technical Background

Small satellite systems ("smallsats": nanosats, CubeSats, and other small spacecraft) have reached a point in their technological evolution in which they are capable of supporting significant scientific investigations. CubeSat missions in low Earth orbit (LEO) have begun to produce valuable science results. The relevant technologies are now being pushed to enable smallsat missions beyond LEO [*Staehle et al*., 2013]. The first beyond-Earth CubeSats were selected by NASA in the fourth round of the CubeSat Launch Initiative. The Interplanetary NanoSpacecraft Pathfinder In Relevant Environment (INSPIRE) project, built at JPL, will demonstrate functionality, communication, navigation, and payload-hosting in interplanetary space on dual 3U CubeSats scheduled to launch July, 2014 [*Klesh et al*., 2012]. The capability to send CubeSat-sized spacecraft to the Moon and its vicinity to make useful measurement is expected to arrive soon, based in part on hoped-for results from INSPIRE, and from multiple subsystem-level efforts at universities and small businesses around the US and beyond.

Small spacecraft to date, including CubeSats (Fig. 4), have enabled space experimentation and technology development on an accelerated schedule for comparatively low cost. Small satellite missions facilitate valuable opportunities to test emerging technologies and economical commercial off-the-shelf components that may be useful in future, larger-scale space missions. Using CubeSats (1.3 to 4.0 kg satellites so far, soon to increase to a maximum of 10-12 kg using a 6U form factor), NASA has tested innovative science and engineering technologies on a smaller scale in the space environment to better understand how hardware will survive the radiation, temperature and vacuum conditions encountered in space. NASA smallsats are designed for a wide spectrum of space missions including biology experiments, testing advanced propulsion and communications technologies. To date, NASA centers have led 6 successful CubeSat missions and the smallsat community has flown over 100.[1] Two recent cluster missions in November 2013 launched 31 CubeSats (ORS-3 from NASA's mid-Atlantic launch range at Wallops Island, Virginia) and 29 smallsats (Kosmotras mission from Yasny, Russia).

Figure 4: Three CubeSats in low-Earth orbit just after deployment from the International Space Station (Credit: NASA)

A number of factors have contributed to this rapid expansion, including: advances in microelectronics and microcontroller/microprocessor technologies, less expensive and more accessible satellite technologies (i.e. commercially available subsystems), the evolution of advanced small detector technologies, and increased satellite launch opportunities thanks in part to the commercialization of space, and overt Government policy to make CubeSat launch slots available on DOD and NASA launches. CubeSat technology has now evolved to the point where valuable science research is supported; for example, CubeSat missions are beginning to contribute to our understanding of space weather, the aurora, the ionosphere, microbursts in the Earth's radiation belts, the Earth's radiation budget, and a variety of astrophysical phenomena. Many more such missions are planned, one of many examples being Morehead State University's Cosmic X-Ray Background Nanosatellite-2 (CXBN-2, following CXBN launched in 2012), with which author B. Malphrus is affiliated.

[1] NASA CubeSat missions to date include: GeneSat, PharmaSat, Pre-Sat, O/OREOS, NanoSail D, PhoneSats. NASA is partnered with universities on several other missions, including COVE, COVE-2, and IPEX with JPL and GSFC.

The importance of smallsats and the CubeSat form factor is evidenced by the success of these missions and by the establishment of NASA's Office of the Chief Technologist (OCT; now Space Technology Mission Directorate (STMD)) Small Spacecraft Technology Program. Smallsat programs directly align with OCT's Space Technology Program (STP) whose purpose is to advance broadly applicable technology to infuse solutions into applications for which there are multiple customers. The OCT/STMD Edison program selected three technology development missions now in development: Integrated Optical Communications and Proximity Sensors for CubeSats, led from Aerospace Corporation; Integrated Solar Array and Reflectarray Antenna (ISARA) for High Bandwidth CubeSat, led from JPL; and Proximity Operations Nano-Satellite Flight Demonstration, led from small business Tyvak Nano-Satellite Systems LLC. The Small Spacecraft Technology Program has three primary objectives, two of which are directly addressed by small satellite missions:

1. *Identify and support the development of new subsystem technologies to enhance or expand the capabilities of small spacecraft*
2. *Support flight demonstrations of new technologies, capabilities and applications for small spacecraft.*

The program seeks to demonstrate technologies that are new and capabilities that have not previously been demonstrated in space.

Smallsat technologies are under development to support missions to Lunar Orbit and to the inner solar system utilizing these small, rapid development and cost-effective form factors. Meanwhile, contracting budgets for scientific research can no longer support numerous major satellite programs to lunar destinations and beyond. With the advent of micro and nanotechnologies and the evolution of these small, inexpensive satellite platforms, Solar System exploration may undergo a new revolution.

3 Study Program Elements

The *New Approaches to Lunar Ice Detection and Mapping* study consisted of two workshops and a three-month intervening study period. Both workshops were held at the KISS facilities on the Caltech campus. As in previous KISS studies, the goal was to conduct in-depth discussions and develop new mission concepts with the potential for revolutionary scientific advancements or technological innovations. The invitation-only workshops (July 22-25 and Nov. 4-7, 2013) involved more than 30 core participants hailing from 16 separate institutions, including 5 NASA centers and 7 universities. Three study Co-leads (P. Hayne, D. Paige, and A. Ingersoll) directed the technical aspects of the study, along with the Distinguished Visiting Scientist (W. Feldman). Within this relatively small group, expertise spanning a range of disciplines including planetary science, lunar exploration, engineering and technology allowed creative thinking, in-depth discussions, and analysis of a wide range of possible measurements and mission designs. Prior to the start of the first workshop, we held a public one-day short course to introduce participants and the community to lunar science and small satellite technologies.





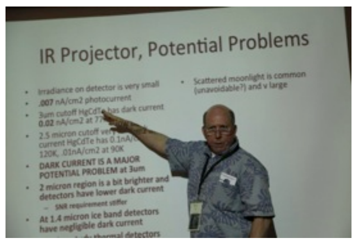


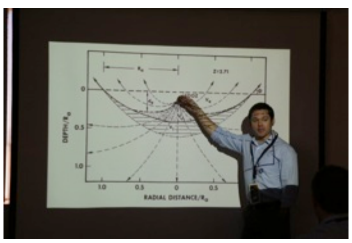

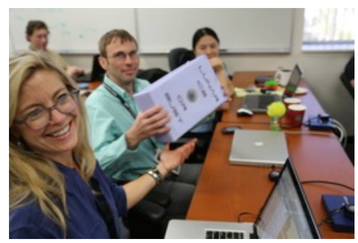



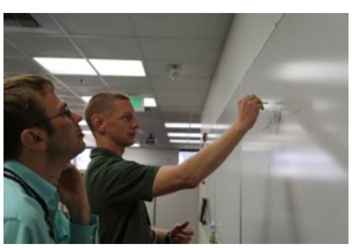
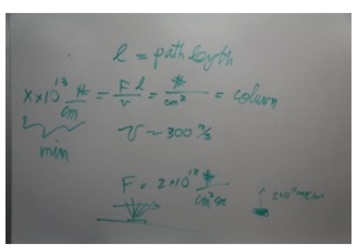
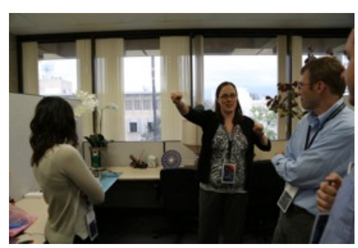

4 Study Results

4.1 Roadmap for Volatiles Investigation

The detection, characterization, and mapping of water ice in the lunar polar regions represents a key step in the broader study of volatiles in the inner Solar System. We envision a possible timeline for the science and exploration of volatiles (Fig. 5), guided by two questions:

1. *What are the origins and evolution of water in the inner Solar System?*
2. *Where are the operationally useful volatile deposits for Solar System exploration?*

Although the order of discoveries cannot be known in advance, the timeline generally progresses in the order of increasingly sophisticated (though not necessarily more costly) remote sensing investigations, toward *in situ* extraction and analysis, and returned samples. The notable exceptions are the Apollo samples, which continue to reveal a great deal about the nature of lunar volatiles decades after their return (Section 4.5), but which did not come from the polar regions. This timeline also includes a bifurcation point, where the most effective probes for the scientific study of volatiles diverge from those best suited for exploration purposes. We envision this bifurcation occurring once a key set of measurements are made:

Measure the concentration of water ice in the upper few meters with sensitivity better than 0.5wt% at multiple locations with diverse thermal environments

Both the science and exploration of lunar volatiles will benefit from prioritizing this measurement goal. Once this set of measurements has been acquired, focused investigations for science and exploration may be more fruitful for each. Nonetheless, future missions should continue to leverage synergistic information between the science and exploration halves of this endeavor. For example, although the isotopic composition of lunar water ice may appear irrelevant for *in situ* resource utilization, the information this provides about volatile origins and transport history would likely guide the search for the most concentrated resources. How close are we to this bifurcation point? In the following sections, we argue that these key measurements are readily attainable, and should be the highest priority in addressing outstanding questions in the science and exploration of lunar volatiles.

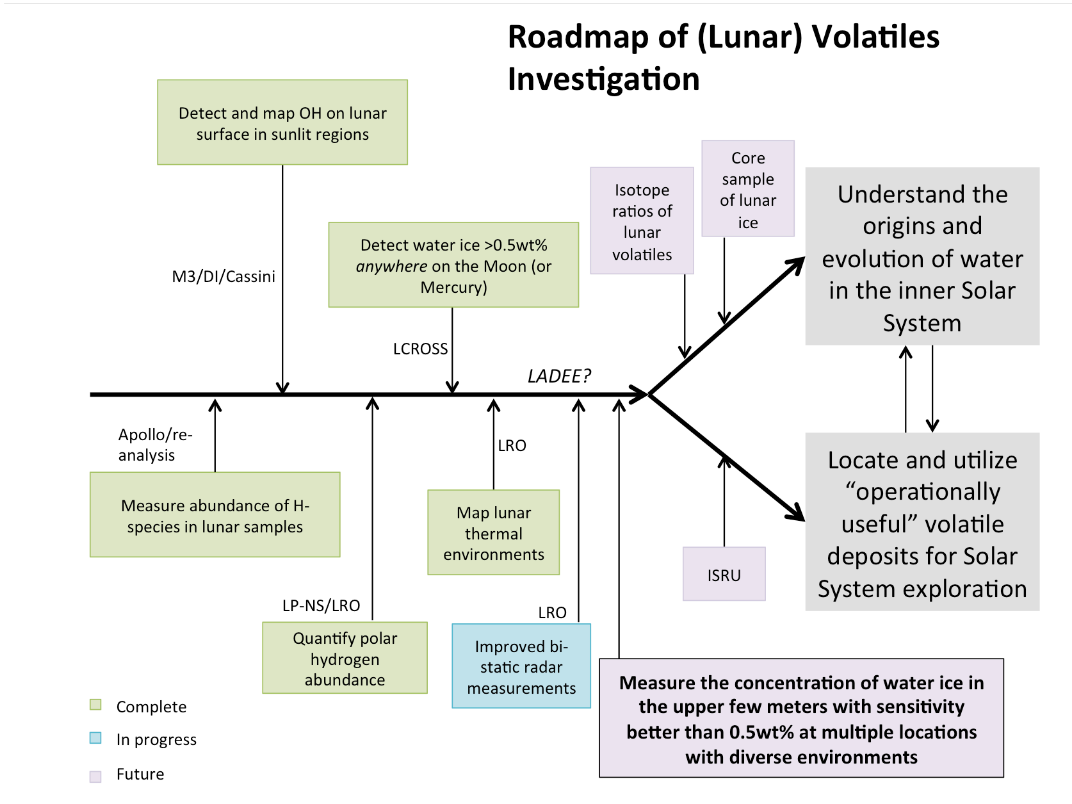

Figure 5: Roadmap for the science and exploration of volatiles on the Moon and beyond.

4.2 Outstanding Questions

4.2.1 Science

The science of lunar volatiles suffers from a great deal of confusion as to what questions remain unanswered. Popular opinion appears to be that we either know there is abundant ice on the Moon (as per the LCROSS results) or that the Moon is essentially devoid of *highly concentrated* deposits of water (which is consistent with radar and neutron data sets, especially as compared to measurements of the planet Mercury). In reality, the scientific community appears to have little consensus as to the location, quantity, and origin of volatiles on the Moon. Here we attempt to provide a roadmap of questions, unanswered and answered, to guide future exploration and lunar volatiles research.

The initial question: **"Is water present on the Moon?"** was reopened in 2008 with laboratory detection of lunar water within returned volcanic glasses [*Saal et al.*, 2008]. Before this point, lunar water remained only a theoretical construct, most likely to be found in shadowed regions near the lunar poles [e.g., *Watson et al.*, 1964;

Gibson and Moore, 1973; *Arnold*, 1979]. The 2009 M^3 instrument confirmed at least OH was widespread [*Pieters et al.*, 2009], and the LCROSS mission was able to verify the prediction of water ice near the lunar South Pole [*Colaprete et al.*, 2010].

Answering the existence question has now led to more nuanced questions of **"What is the geographical extent, quantity, and origin of this water and other volatiles?"** Recent confirmation of the presence of water does not yet answer these more detailed questions. Here we briefly subdivide these general questions into:

What is the geographical extent of volatiles on the Moon? As discussed in Section 2.1.2, several orbital data sets indicate signs of near surface hydrogen, but these datasets are often non-unique identifiers of water or, in many cases, derive distributions disparate from each other. Thus, the existing datasets have yet to offer a definitive map of near surface water, though some steps toward this question have been made, especially mapping of the global 3-µm absorption feature and mapping of neutron depletion regions near the poles. Sub-questions of this topic are:

- *i) Does the 3-µm absorption feature indicate water in sunlit regions of the Moon? Or is this hydroxyl (OH) only?*
- *ii) Does surface water exist in areas of permanent shadow?*
- *iii) What is the geographic distribution of subsurface water?*
- *iv) Is the presence of water thermally controlled?*
- *v) Are other volatiles present?*

What quantities of water exist on the Moon? Despite its ill-understood geographical distribution, water appears to be present both at the lunar surface, and at depth. Water abundances reported for the LCROSS impact site are at least a factor of ~2 higher than those derived from Neutron Spectrometer (NS) data for the same region [*Colaprete et al.,* 2010; *Feldman et al*., 2001]. Because LCROSS excavated to several meters depth, whereas neutron detectors probe the upper ~1 meter, this discrepancy may imply ice concentrations increase with depth or that ice dramatically varies in concentration laterally at a scale smaller than the NS footprints (< ~50 km). Sub-questions of this topic are:

- *i) Is surface ice present in "useful" quantities for in situ science and resource utilization (here we assume this to be >0.5wt%)?*
- *ii) Do higher concentrations of ice exist at depth?*

What form does water take on the Moon? Water and OH detected at the lower latitudes based on the 3-µm absorption likely takes the form of adsorbed molecules (chemisorbed or physisorbed) on regolith grains [*Poston et al*., 2013], or as indigenous water incorporated in glasses and nominally anhydrous minerals [*Saal et al.*, 2008]. In the polar regions, if ice exists in measureable quantities on or below the lunar surface, we lack detailed understanding of the form it might take. This is greatly dependent on and may be diagnostic of the mechanism by which it was emplaced- i.e. vapor diffusion [e.g., *Schorghofer,* 2007] vs. impact burial [e.g., *Crider and Killen*, 2005]. Neutron and radar data seem to refute Mercury-like solid ice deposits near the surface, but data below ~2m is unavailable [*Feldman et al.*, 2000; *Campbell et al*., 2006].

i) Do ice deposits exist in distinct layers of porefilled regolith?
ii) Does ice form monolayers on grains or fill intergrain voids? (Fig. 6)
iii) Does ice migrate through the regolith in response to temperature gradients? Or is ice concentration dictated by impact gardening mixing?
iv) Are there small ice lenses or concentrated ice layers from past comet impacts?

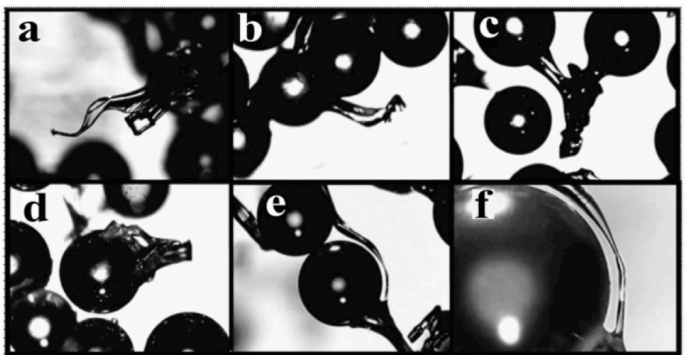

Figure 6: Microscopic images showing examples of ice microstructures formed after 11 hours of vapor deposition on ~500-µm silicate spheres (from: Siegler et al., 2012)

What is the origin of the water on the Moon? Given that ice exists in measurable quantities, knowledge of its distribution (both geographic and as a function of depth) and physical properties may provide information about its origin. Young (or mobile) ice should not be mixed into the regolith. Exogenic ice should be in greater concentrations near to the surface, whereas endogenic water might be concentrated at depth. Isotopic composition (namely D/H ratios for water) can provide strong constraints on origins [*Yung and Dissley*, 1992] and can be aided by measurements of concentration of other volatiles and their isotopic ratios. Sub-questions of this topic are:

i) Does the ice distribution imply a young or ancient ice deposit?
ii) Does the ice distribution imply a source region (from above or below)?
iii) What is the isotopic composition of lunar water and OH?
iv) Do isotopes vary with location and depth?
v) What other volatiles are found and what are their isotopic compositions?
vi) Is the regolith composition distinct/altered in the vicinity of the ice?

Collectively, these questions address a more fundamental planetary science question: what was the origin and evolution of water in the inner Solar System?

4.2.2 Resource Utilization

In Situ Resource Utilization (ISRU) involves processes and operations to locate, harness, and utilize resources in space to create products that can then be used to reduce the mass and cost of human exploration, reduce mission risk by enabling self-sufficiency, and increase performance or enable new mission concepts compared to bringing everything from Earth. Mission architecture studies for the Moon and Mars have shown that the production of mission consumables such as oxygen, water, and fuels for life support, radiation shielding, fuel cell power, and propulsion system applications can have a significant mass, cost, and risk reduction benefits for human missions. While the existence of water and other volatile resources (H_2, CO, CO_2, HN_3, CH_4) at the poles of the Moon has been proven from missions such as LCROSS and LRO, there are three questions that need to be answered before they can be considered viable as a resource for ISRU in human exploration:

ii) *What are the volatile resources at the poles and how are they distributed at the local level?*
iii) *What are the regolith and environmental factors that impact resource acquisition and processing?*
iv) *Is the resource 'operationally' useful for future missions?*

In a similar manner to scientific investigations, characterizing and mapping polar volatile resources involves determining the abundances, the areal and vertical distribution, and the hetero/homogeneity of these resources. It is also important to understand other constituents that may contaminate polar volatile resources of interest (such as Hg, H_2S, SO_2) or degrade resource processing equipment during operation (such as processing byproducts: HF, HCl). Because operations associated with mining polar volatiles will occur over months or years, it is critical to understand environment impacts such as temperatures, illumination, and radiation environments, as well as regolith physical/mineralogical properties on resource extraction and processing hardware. Whether polar volatiles are operationally useful is not only a function of their concentration, distribution, and the location and environment in which they are found. The utility of volatiles also depends on what hardware and infrastructure is required to extract, store, and transport the products from polar volatiles, on how much of the final product is needed, and on how often the products are needed. From this information, an economic return on investment assessment for developing, delivering, and operating ISRU equipment to mine polar volatiles can be made. Because oxygen can be extracted from lunar regolith at an extraction efficiency of 1 to 2% by mass of bulk regolith processed anywhere on the lunar surface, it is tentatively believed that a concentration of at least 0.5% of water by mass within the top 1 meter is required to be considered operationally useful to future missions [*Sanders*, 2013].

4.3 Measurement Strategy

4.3.1 Key Measurements Needed

Addressing the key questions listed in Section 4.2 requires, in priority order: Direct detection of the water molecule; quantification of the abundance of water; detection of other relevant volatile species; understanding the isotopic composition of the detected volatiles, including water ice in order to understand the origin and evolution of the deposit. Important ancillary measurements might include the composition (chemistry and mineralogy) of the regolith in contact with the ice. In

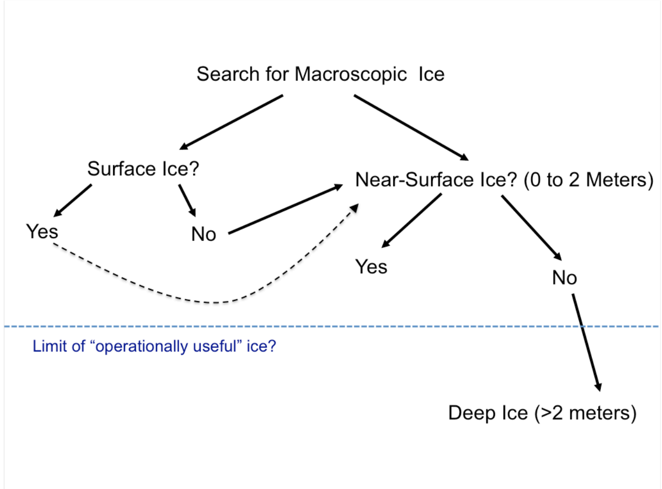

Figure 7: Strategy for detecting and mapping lunar ice deposits.

addition, the geographic distribution of H_2O and other volatiles should be constrained, if not mapped.

Two general methods are available for direct detection: observations of the undisturbed lunar surface exploiting the spectral properties of water ice and hydrous geologic materials or active excavation of lunar material through landed missions with drilling/excavation or artificial impacts such as demonstrated by LCROSS that provide access to the shallow subsurface and additional spectral phenomena not available to surface measurements (such as gas phase spectroscopy).

The advantage to observations of the undisturbed surface is the synoptic reach of these measurements; comprehensive surveys of the polar regions are possible. Water ice exhibits diagnostic spectral features from the ultraviolet to the far infrared. The very strong OH and water ice fundamentals near 3.0-3.1 µm and their combination and overtones near 1.-1.5 µm and 1.9-2.0 µm have been well-characterized in terrestrial laboratories and detected on other planets. The ultraviolet also features a water absorption near 165 nm wavelength, though experimental challenges have led to fewer laboratory data supporting full understanding of the phenomenology. Mid-infrared spectra have hydration and water ice features near 6.0 and 12 µm. Least well studied is spectroscopy of water ice bands the far-infrared between 40 and 60 microns but understanding the spectral properties of ice vs. hydrated materials in this region may yield important diagnostic spectral features (see Section 4.4.4).

Extracting actionable isotopic information from passive measurements appears not to be practical at the surface concentrations of ice anticipated, and it has not been demonstrated. Such information is accessible using vapor phase spectroscopy or in-situ mass spectroscopy enabled by artificial impacts. Microwave measurements of gas released by an artificial impact are particularly attractive in this role because of their high sensitivity to oxygen isotopes via rotational transitions (Section 4.4.6).

4.4 Remote Sensing Techniques

We studied a number of techniques for detection of H_2O and other volatiles on the Moon; in this section we focus on the most promising types of measurements for future missions. The table below summarizes several of these techniques, which are described in detail in the following sections.

Table 2. *Comparison of measurement techniques for ice detection and characterization*

Technique	Depth sensed	Detection limit on H_2O	Heritage
UV	~1 μm	< 0.5wt%	LRO LAMP
Shortwave-IR	~10 μm	~10 ppm	M^3
Thermal-IR	~1 – 10 mm	*Unknown*	LRO Diviner
Neutron/gamma ray	~1 m	~100 ppm [H]	LPNS, LEND
Radar	~1 – 10 m	Macroscopic blocks	LRO mini-RF
Passive microwave	Impact vapor plume	$\sim 10^{13}$ H_2O molecules cm^{-2}	Rosetta/MIRO
In-situ gas analysis	Drill/mole	< 1 ppb/g soil	MSL/TLS, Huygens GCMS

4.4.1 Ultraviolet

Ultraviolet spectroscopy is a remote sensing technique that can be used to sense H_2O ice at the Moon, utilizing the strong H_2O absorption edge near 165 nm. The Lyman Alpha Mapping Project (LAMP) [*Gladstone et al.*, 2010] on LRO is a key example of the utility of UV spectroscopy for this purpose. LAMP has been used to detect lunar H_2O ice at abundances as low as ~0.5-1%, in polar PSRs [*Gladstone et al.*, 2012] and on the dayside [*Hendrix et al.*, 2012], at depths on the order of microns into the regolith.

At the workshop, we discussed that UV spectroscopy can be performed from an orbiter using passive and/or active illumination sources. For passive sources, UV spectroscopy can use solar light (as is used for dayside observations by LRO/LAMP) or stellar/interplanetary hydrogen (IPH) sources, as is used for night side and PSR regions by LAMP. UV spectroscopy can also be used to measure, from orbit, gases (e.g., OH, H_2O, H) released in impactor plumes.

Possibilities for near-future UV instrumentation to improve upon LAMP measurements include miniaturization of components, increase of detector sensitivity and a simplification of LAMP for the exclusive detection of H_2O ice (e.g. a two band imager).

4.4.2 Radar

Radar systems transmit a radio signal towards a target and receive its return. Unlike passive forms of remote sensing, which rely on external light sources, radar systems are active and use their own transmitting system to illuminate a surface. Earth-based radars have been mapping the Moon since the 1970s, but the synchronous rotation of the Moon prevents ground-based observers from observing the lunar far side, and much of the polar regions. The first imaging radar systems to orbit the Moon were launched in 2008 and 2009, on board the Chandrayaan-1 and LRO spacecraft. Over its lifetime, Mini-RF on LRO imaged > 98% of both poles down to 70°. Given the low altitudes and orbital velocities at which a lunar radar can operate, Mini-RF is a relatively small radar, with a mass of only 14 kg and an antenna area of ~1 m^2 [*Raney et al*., 2011].

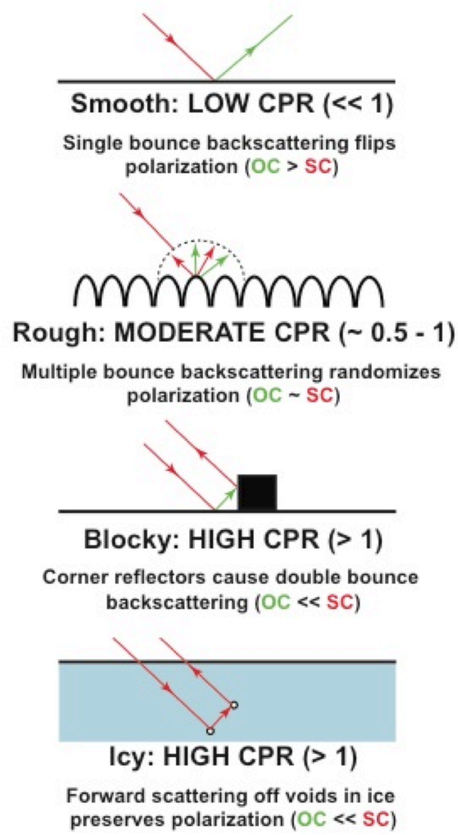

Figure 8: Comparison of radar scattering for rocky vs. icy surfaces.

Radars are capable of penetrating to the near subsurface, and could observe ice at the lunar poles even if it is buried under regolith. For a typical wavelength of 12.6 cm, a radar system could detect ice deposits a few meters down. However, these tests will only be effective if the ice is present as a thick deposit (~10 λ) of nearly pure water ice. If water is present in the form of small grains of ice mixed into the regolith, it will be difficult to distinguish from a rocky surface, since the change in dielectric constant caused by the presence of a small concentration of water ice would not produce large scattering differences [*Thomson et al*., 2011].

Radar systems have two main advantages over passive spectroscopy/radiometry for detecting water ice near the poles of the Moon. First, they are capable of seeing into permanently shadowed regions. Second, cold water ice is known to have unique radar properties. The Galilean satellites [*Ostro et al*., 1992], Mars' polar ice caps [*Muhleman et al*., 1991], and the permanently shadowed regions on Mercury [*Harmon et al.*, 2011; *Chabot et al.*, 2012] all have large same-sense radar reflectivities and circular polarization ratios that exceed unity. These properties are unusual compared to most targets in the solar system, and are thought to be indicative of the coherent backscatter effect in thick deposits of cold water ice. The coherent backscatter effect leads to large returns in the same sense (SC) polarization and values for the circular polarization ratio (CPR) that can exceed unity. However, the presence of high circular polarization ratios can be explained through other mechanisms that do not require the presence of water ice [*Campbell*, 2012] (Figure 8). This ambiguity can be resolved through bistatic radar measurements, where the transmitter and receiver are physically separated. This is because the coherent backscatter effect relies on positive interference at low bistatic angles, so unlike rocky surfaces, the radar return should drop rapidly at bistatic angles much larger than zero. Bistatic observations are currently underway using the Arecibo transmitter and the Mini-RF receiver on LRO [*Bussey et al*., 2012].

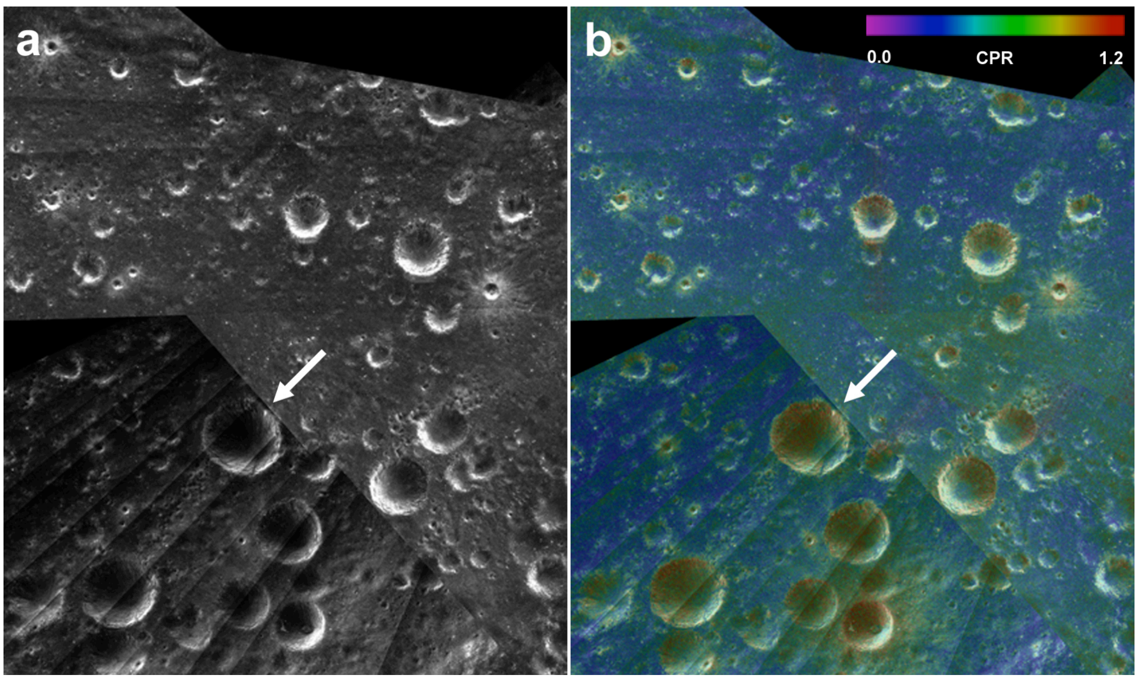

Figure 9: Several small craters within Peary crater, near the lunar north pole, have high CPRs within their crater rims, but lack the bright ejecta blankets associated with young, fresh craters. This is consistent either with the presence of ice, or rough, blocky crater walls. Shown here is (a) total radar backscatter as observed by Mini-RF on LRO and (b) circular polarization ratio overlaid on total radar backscatter, scaled from 0 (purple) to 1.2 (red)."

4.4.3 Shortwave-IR

Shortwave-infrared reflectance spectroscopy, defined here to be wavelengths from 1.0 to 5.0 μm, is used routinely to identify and map water ice on planetary surfaces. It is also used to distinguish non-ice constituents or impurities within water ice at a ~1% level. Shortwave-infrared reflectance spectroscopy has been used to study the Martian polar caps [e.g., *Langevin et al*., 2007], Martian mid-latitude and polar "dirty ice" deposits [e.g., *Langevin et al*., 2005a; *Calvin et al*., 2009], Jovian satellites [e.g., *Hansen and McCord*, 2008], and Saturnian satellites [e.g., *Brown et al*., 2006] from orbiting instruments and telescopes [*Emery et al*., 2005]. Water ice can be clearly distinguished from hydrated (H_2O) or hydroxylated (OH) silicate surface materials by the position of characteristic absorption minima at 1.5, 2.0, and 3.1 µm in the former and at 1.4, 1.9, and 2.7-2.9 µm in the latter. The breadth of these absorptions in water ice is also considerably greater than that in hydrated/hydroxylated mineral surfaces (Figure 10).

As discussed further in 4.5.2, the detection threshold for water ice in regolith is dependent on both the details of the radiative transfer modeling used as well as assumptions about the grain size and optical properties of the non-water ice materials. Band strengths of ~10% at 3 um and ~1% at 2um may be anticipated for a suite of plausible regolith types with particles of water ice at ~0.5 wt. %.

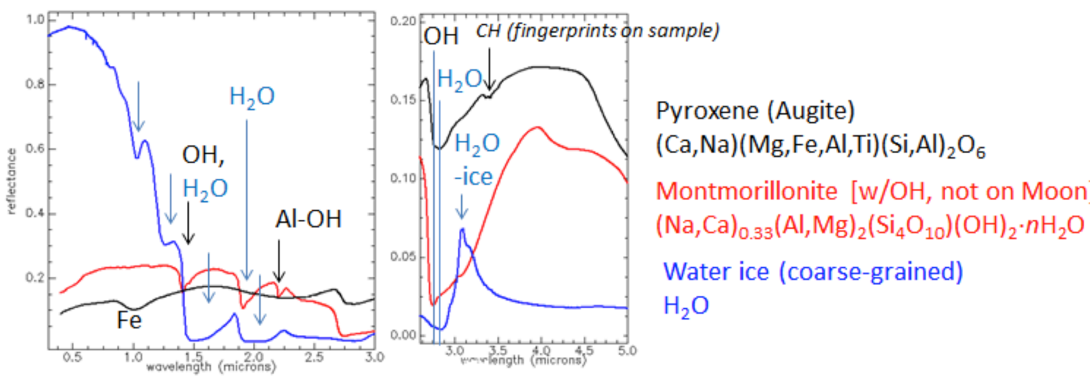

Figure 10: Shortwave infrared spectra of nominally anhydrous silicate (with trace OH) (black line), hydrated/hydroxylated silicate (red line), and water ice (blue line). These spectra demonstrate how water ice is clearly distinguishable from anhydrous and hydrated silicates.

To date, the wavelength coverage of shortwave-IR data on the Moon has not covered the 3.1-µm absorption line for water ice. Moreover, nearly all putative ice detections on the Moon are in permanently shadowed regions. Without active illumination, there is insufficient signal (given current sensor technology) to detect spectral features of ice. In situ or active remote sensing (see 4.4.6) will be necessary to utilize this highly sensitive wavelength region for lunar ice detection.

4.4.4 Thermal-IR

The use of thermal infrared spectroscopy, defined here as wavelengths from 5.0 to 500 µm, for water-ice detection in predominately dusty planetary regolith has thus far not been utilized. However, the technique has been well demonstrated for atmospheric, comet, and icy satellite observations [*Pearl et al*., 2001; *Ootsubo et al*., 2009; *Howett et al*., 2010]. There are water-ice vibrational absorptions across the mid-IR (6 µm and 12 µm) to far-IR (45 µm and 62 µm) that can be used to unambiguously detect water and water-ice [*Maldoni*, 1998; *Moore and Hudson*, 1992]. However, in the presence of fine-grained silicates, the far-IR band at 45-55 microns is most likely to yield a detection. Any detection would be limited to the surface boundary layer (~ millimeter deep).

This far-IR band is sensitive to crystallinity, grain size, dark contaminants and porosity of water ice [*Carvano et al*., 2006], which increases the utility of the observation but also increases the complexity of the measurement (more channels are required to capture all possible modes). This complexity can be decreased if the mostly water-ice structure and composition can be constrained for an individual body. Detection would be possible in both day and night, however, it is expected that surface water ice will only be present in permanently or near-permanently shadowed regions.

The Diviner Lunar Radiometer, flying onboard LRO, has 9 infrared channels with wavelengths from 0.3 to 400 μm [*Paige et al*., 2009], and the likely required sensitivity to make this detection. Unfortunately, Diviner lacks spectral filters at the appropriate wavelengths. A re-fly of a modified Diviner, or simpler instrument designed for a CubeSat, has the potential to make this water-ice detection.

4.4.5 Neutron and Gamma Ray Methods

Remote sensing of neutrons and gamma rays has been established as a standard remote sensing technique in planetary geochemistry research to observe regional hydrogen concentrations. Missions that have used these techniques include: Lunar Prospector Neutron Spectrometer (Neutron and Gamma-ray), Mars Odyssey (Neutron and Gamma-ray), Lunar Reconnaissance Orbiter (Neutron) and Mercury Messenger Neutron Spectrometer (Neutron and Gamma-ray) [*Feldman et al*., 1998; *Boynton et al.*, 2004; *Mitrofanov et al.*, 2010; *Lawrence et al.*, 2012]. In-situ active neutron methods use a radioisotope source to produce energetic neutrons that interact with H in the surrounding regolith. This method has been developed for the Mars Science Laboratory (MSL), Dynamic Albedo of Neutrons Detector system [*Litvak et al.*, 2011].

Passive techniques:
Orbital techniques rely on galactic cosmic ray-induced production of neutrons and gamma rays from regolith. The energy distribution of neutrons and gamma rays as leakage fluxes coming from any airless planetary body is dependent on the influx of galactic cosmic rays (GCR) that spall neutrons and gamma rays in the top meter of regolith. Fluences of characteristic gamma rays are used to determine the elemental compositions of regolith [*McKinney et al*., 2006]. GCR flux rates are nearly isotropic and their rates are inversely related to the solar cycle (i.e. heightened solar plasma fluences attenuate the influx of GCR into the solar system). GCR rates and the dependent leakage fluxes are independent of day/night temperature variations and have been the primary detector systems used to probe hydrogen abundances in the near sub-surface of the Moon's PSRs.

Neutron energies are described as follows: thermal (0.025 to 0.4 eV), epithermal (0.4 eV to 1 MeV), fast (1 to 20 MeV). All neutron energies are to some degree sensitive to hydrogen, but epithermal neutrons are the most sensitive to H its high cross-section to neutrons in that energy range [*Feldman et al*., 1999; *Lawrence et al*., 2013]. Neutron count rates are proportional to the cross-section of the detector systems to the incoming leakage fluxes. Due to the typically low count rates, multiple flyovers are required to collect statistically significant results. From 50 km altitude, LPNS spatial resolution was ~45 km, LRO LEND was ~10km. Such techniques have sensitivities ~100 ppm H. Similar rates and resolutions are required for orbital detection of gamma rays [*Mitrofanov et al*., 2010; *Maurice et al*., 2004].

4.4.6 Passive Microwave

Passive microwave radiometry and spectroscopy are potentially revolutionary tools for the exploration of near surface lunar volatiles. "Passive microwave" here is loosely defined as wavelengths from tenths of millimeters (~1000GHz) to tens of centimeters (~1 GHz), and is distinguished from radar by not using an active transmitter. Long wavelength microwave radiometers (~1-30 cm) have been suggested as a tool for exploring the subsurface structure and interior heat flux of planetary bodies [*Kiehm*, 1984]. These instruments recently orbited the Moon on two Chinese missions operating at 7.8, 19.35, and 37.0 GHz [e.g., *Fa*, 2010]. Short wavelength microwave radiometers (<1cm) are a relatively new technology. These instruments are especially applicable to the identification of the rotational and translational bands of water [*Gulkis et al*., 2007].

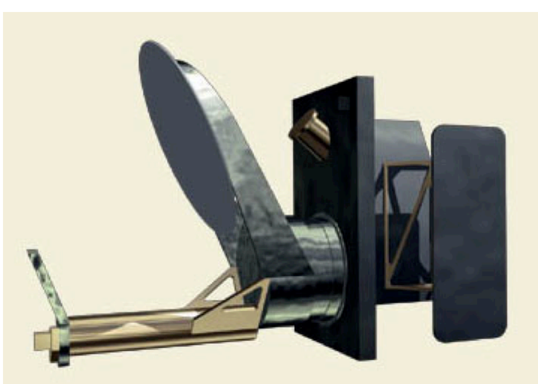

Figure 11: The MIRO microwave spectrometer developed and built at JPL (Credit: NASA/Caltech)

Long wavelength thermal emission spectrometers, like those flown aboard the Juno mission (at 0.6, 1.25, 2.6, 5.2, 10, and 22 GHz, or 1.4 – 50 cm) have been designed to probe different depths of planetary atmospheres. Likewise, such instruments can be used to explore solid body sub-surfaces, depending on the electrical attenuation properties of the subsurface material. For lunar regolith, a microwave radiometer can probe roughly 5 to 10 times the wavelength used [*Keihm*, 1984]. If buried ice were to exist in large enough quantities to effect electrical attenuation length or thermal properties (by filling pore spaces otherwise filled by vacuum), long wavelength measurements should be sensitive to fairly small quantities of buried ice. The primary limits of such instruments are resolution (likely > 1 km from lunar orbit), unknown scattering effects, size, and mass (such antennas are on the order of 10x the wavelength).

Short wavelength instruments can be much more compact, but penetrate only the very near surface. The Microwave Instrument for the Rosetta Orbiter (MIRO) instrument (at 190GHz and 562 GHz, or 1.6 and 0.53 mm) has successfully characterized the very near surface regolith (top 1cm) of several asteroids on its approach to a comet as part of the Rosetta mission (Fig. 11). Similar to the long wavelength instrument, this type of remote sensing could likely show density and dielectric property anomalies (such as near surface pore-filling ice).

Microwave spectrometry allows extremely high sensitivity: the Rosetta MIRO instrument requires a minimum column abundance of ~10^{13} water molecules per cm^2 [*Gulkis et al*., 2007], compared to ~10^{15} molecules per cm^2 detected by LCROSS [*Colaprete et al*., 2010]. The MIRO instrument also employs a 4096 channel spectrometer to extend each of these channels by +/- 90 MHz with ~44 kHz resolution [*Gulkis et al.*, 2010]. Such spectrometry is particularly useful in that it allows for extremely high sensitivity of molecular isotopic species, including $H_2{}^{16}O$, $H_2{}^{17}O$, and $H_2{}^{18}O$ when in a vapor form (Fig. 12). Therefore, this measurement excels in finding volatiles if they have been liberated in an LCROSS style impact. The principal advantage of such an instrument is that it requires no illumination of the impact plume, allowing it to be small and in permanent shadow. Similar instruments have also been developed for CubeSat deployment, such as the MicroMAS spectrometer, launching in early 2014 [*Blackwell et al.*, 2013].

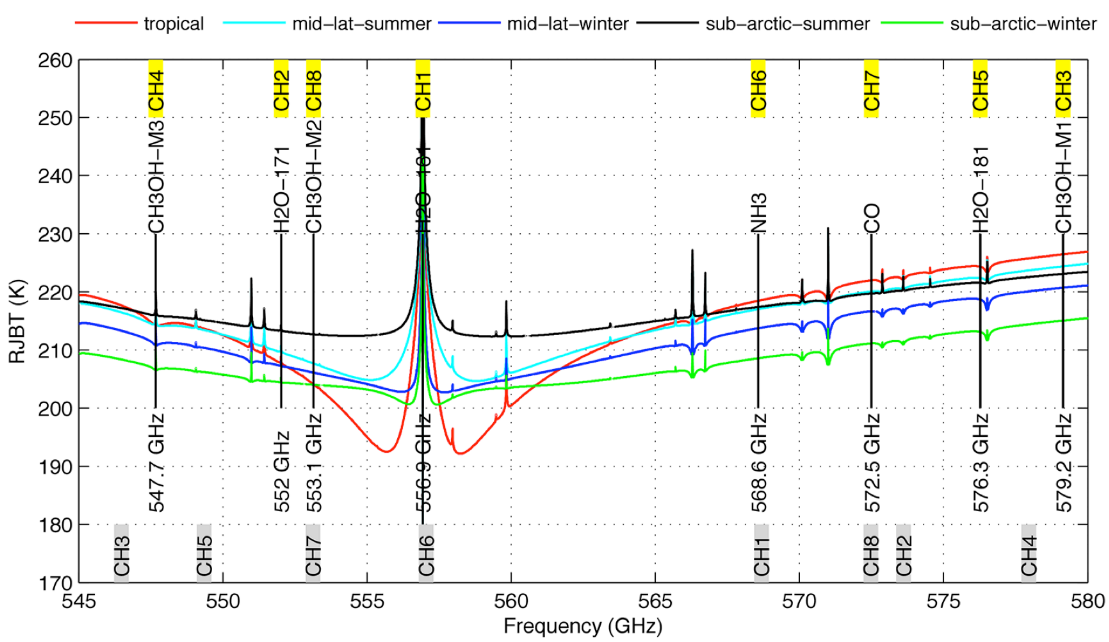

Figure 12: Microwave emission spectra of Earth, acquired by MIRO on the November, 2007 Rosetta flyby. Several important atmospheric species exhibit absorptions in this spectral range, in addition to H_2O. Adapted from: Jiménez et al. *[2013].*

4.5 In Situ Measurements

4.5.1 Sample Analysis

In-situ sample analysis can provide definitive identification of H-bearing species and their origin. In-situ sampling also determines the spatial distribution, physical/chemical state, and abundance of water at a fine scale, which is important for in-situ resource utilization. Present data from different remote-sensing instruments provide ambiguous results, providing further motivation for the investigation of lunar volatiles by in-situ techniques (Section 4.2). A surface mission requires landing site precision and mobility at a relatively small spatial scale (~1 km to target diverse thermal environments), should collect and deliver samples from depth (a few meters), and have the ability to determine volatile origins, species, and abundances. Here we document the instrumentation available for in-situ analysis.

The isotope values of hydrogen and associated volatiles (e.g., N) provide robust but non-unique identification for the origin of water. Hypotheses for the origin of lunar polar ice include solar wind, magmatic water, chondritic (meteorite) input, or comet impacts. However, isotope values of H, N, and O of these potential sources are distinctively different only between solar wind and cometary sources (Fig. 13) [*Marty et al*., 2011; *McKeegan et al*., 2011]. Chondrite, lunar mantle [*Saal et al*., 2013], and terrestrial water display insignificant differences in D/H, $^{15}N/14N$, and three O-isotopes. Because chondritic meteorites also supply organics, the ability to

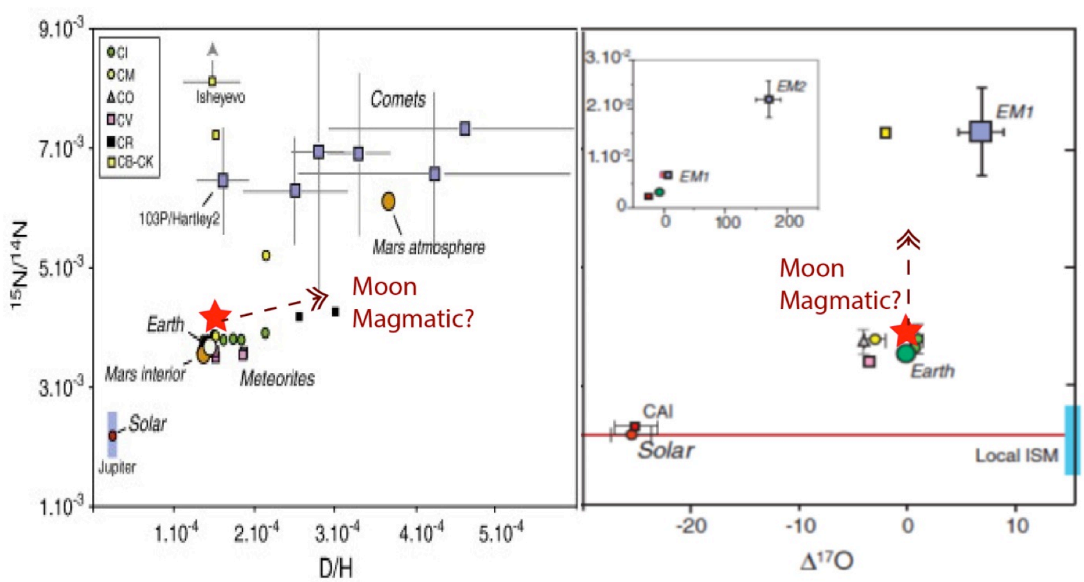

Figure 13: N, H and O isotope composition of the solar system bodies, showing the large variation among solar, chondritic (Earth, Moon), and cometary values. The D/H value of lunar mantle water is from Saal et al. (2013). The magmatic nitrogen was assumed to be those measured in igneous samples (e.g., [Becker and Clayton, 1975]). Oxygen isotope of lunar samples overlaps with terrestrial values [Liu et al., 2010; Spicuzza et al., 2007; Wieler et al., 2000]. These figures were adapted from Marty et al. (2011) and (Marty, 2012).

identify organics will aid the determination of water origin.

There are additional complications that need to be considered for in-situ study. For example, if water ice and organics were derived from different sources but were deposited in different layers, in-situ sampling without a fine-scale imaging could lead to misinterpretations. Additionally, regardless of the source of water, its isotopic composition could be altered by cosmic ray spallation and micrometeorite vaporization. The magnitude of alteration depends on how long the ice was exposed to these effects. Thus, for in-situ sampling, it is also important to be able to determine the exposure history of the ice deposit.

Table 3 summarizes the requirements for in-situ analysis of lunar ice samples. Ideally, these measurements should: (1) determine the abundances and isotope composition of volatiles; (2) identify organics and their isotope composition; (3) provide context and mineralogy imaging as well as fine scale imaging; (4) the exposure/deposition history (in relation to 3). Furthermore, sample collection, delivery, and processing are needed for extracting and delivering volatiles to the analytical instruments.

Table 3: Science traceability for in-situ instruments.

Investigation	Measurements	Requirements
Origin	Isotopes of H N O (C and S)	Difference of 100‰ for D/H (D of ppb moles) Difference of 5-10‰ for 3-O (^{17}O of ~ppb mole)
Origin	Organics	Identify presence and species
Distribution	Abundances; Spatial range	ppmw detection limit Ability for mobility and depth sampling
History	Local context/ geochronology	• Ice crystallinity • Context mineralogy of ice deposit • Geochronology of regolith above or below
Sample processing		Collection (solid, gas), Heating, Combustion with O_2 to produce oxides

Present-day instrumentation for the above-proposed analysis has been well documented in the Science Definition Team report for Mars-2020 project, some of which were flown on MSL [*Mustard et al.*, 2013]. For each measurement (or investigation) in Table 1, there are many choices among flight instruments or instruments in development. These are listed in Mustard et al. [2013], and here we list the flight instruments (proven applicability) in Table 4.

For different instruments, requirement of sample preparation differs:

MS, GC-MS, TLS:

- Sample collection: drill, excavator, scoop
- Oven for volatile extraction
- Pyrolysis in oven (to 110 C) to evolve gases from soil
- Combustion with O_2 from macromolecular C to produce oxides, e.g., CO_2, CH_4
- Liquid derivatization by making non-volatile polar compounds volatile (e.g., amines, carboxylic acids, nucleobases) for analysis by GCMS

Spectroscopic methods (Raman, IR):

- Cleaning surfaces

Table 4. Applicability and sensitivity of flight instruments for in-situ analysis of lunar volatiles.

Technique	Abundances	Isotopes	Complex Organics	Local context	Require sample processing
Mass Spec. (MSL-QMS MSL-GCMS)	√ (5-10% noble gases 5-20% for CH_4, NH_3, H_2O) ~0.6 ppb /g soil	√ H, C, N, O, S (+/-noble gases) (20% D/H in H_2, 1-10% 13C/12C)	(√)	x	Yes
TLS	√ (10^{-10} g_H_2O/g_soil)	√ H, C, N, O, S 0.1% isotope ratios	√	x	Yes (operation at 4-9 mbar)
GC	x	x	√	x	Yes
Neutron Spectro.	√ (bulk) (~0.1-0.3 wt%)	x	x	x	No
Raman (green, UV-)	(√)	x	√	√ (mineralogy)	Clean surface
IR	√	x	√	√ (mineralogy)	Clean surface (Light illumination for permanently shadowed)
APXS	Bulk chem, non-volatiles (100 ppm Na-Ba)	x	x	√ (bulk chem)	Clean surface
LIBs	Bulk chemistry (< ppm for H-Pb, except for 5-10% halogens)	x	x	√ (bulk chem)	Laser source

4.5.2 Active Neutron Detectors

An active pulsed neutron source, combined with neutron and gamma ray detectors could provide ideal capabilities for *in situ*, subsurface detection of H. This instrument system has not flown previously to the Moon, but has precedence in in the oil well logging industry, so has a high technology readiness level. The system can detect sub-surface H down to a meter, detects geochemical layering effects, is non-destructive, does not require mechanical devices and facilitates the detection and quantification of most elements found in planetary regolith.

Active techniques:
Neutron generators, such that employed by Mars Science Lab's Dynamic Albedo of Neutrons (DAN), produce 14 MeV neutrons at 10^8 – 10^9 $n \cdot s^{-1}$ that interact with regolith nuclei up to a meter depth. This technique facilitates the removal spacecraft background, characterization of H sources ($H/OH/H_2 0$), and the discrimination of layering. The exclusive use of neutron detectors limits DAN's application to subsurface H and other elements with high-cross section to neutrons (e.g. Cl and Fe). DAN can detect regolith H content as low as 0.1%. For in-situ analysis, the use of a pulsed neutron source provides approximately 2 orders of magnitude faster accumulation of neutrons and gamma rays compared to passive techniques. Vertical layering resolution is a few cm and horizontal resolution on the rover is ~50 cm [*Litvak et al*., 2008].

Active pulsed neutron source with neutron and gamma-ray detectors:
This ruggedized instrument system developed by Schlumberger Corp. and others has been used for years in oilfield exploration to optimize drilling operations and mineralogical exploration. Presently, this system is under development for use on planetary and small bodies applications by personnel at the Goddard Spaceflight Center's Neutron and Gamma ray test facility [*Parsons et al*., 2011; *Bodnarik et al*., 2013; *Starr et al*., 2007; *Trombka et al*., 2005]. The system provides an extension to the functionality provided by the DAN instrument, but also includes a gamma-ray detector to quantify the sub-surface elemental composition. Several gamma-ray detector systems are applicable and already have high technology readiness levels. The system has several distinct advantages in the detection of H over other methods: 1) non-invasive observation of the regolith that provides sub-surface elemental and mineralogical layering information to a meter's depth. This information also provides elemental and mineralogical context to other higher-resolution instrument systems. 2) The active generation of regolith leakage neutrons and gamma-rays is approximately 2 orders of magnitude faster than galactic cosmic-rays, ~10 mins for most regolith elements (H, C, O, Na, Mg, Al, Si, P, S, Cl, K, Ca, Ti, Fe, Th, and U, many with absolute uncertainties ≤1%. These detection rates facilitate the continuous accumulation of statistics, even on a moving rover. 3) Due to the rapid return of elemental information and the unique view into the

characteristics of the subsurface, results can be incorporated into rover tactical planning processes, similar to visible imagery, to optimize the deployment of other higher-resolution instrument systems or resources e.g. mechanical arm for APXS or (drills, trenchers, power, time), thus enhancing the scientific return of the mission. 4). The inclusion of the gamma-ray detector system can also be used to constrain the relative concentrations of molecular, ionic H_2, H_2O, OH. The detector systems can also be operated in passive mode (without the pulsed-neutron-generator as a default mode) to collect neutrons and gamma rays generated locally by galactic cosmic rays.

4.6 Technical Challenges and Unknowns

4.6.1 Spectroscopy of Ice/regolith Mixtures

4.6.1.1 Experimental Data

Laboratory experiments are key to understanding data returned from orbital and landed spacecraft and to constraining radiative transfer models. Ultimately, laboratory experiments conducted in the conditions analogous to those observed by spacecraft are most valuable.

A plethora of data potentially characterizing lunar volatiles exists, though few of these datasets are able to peer into the permanently shadowed regions. The lack of laboratory measurements in a lunar-like environment makes this a particularly important area of research, as well characterizing ice/regolith mixtures, in combination with changing crystallinity (as the crystallinity of ice can vary greatly with temperature [*Moore and Hudson*, 1992]), and examining the context of the ice (e.g. massive near surface, thin films, pore ice etc.). Table 5 provides a detailed description of existing measurements broken down by wavelengths of interested identified in the study from the Moon and in the laboratory. This table also provides a list of needed laboratory measurements for each wavelength range.

4.6.1.2 Existing Lunar Measurements

The Lyman Alpha Mapping Project (LAMP) [*Gladstone et al.*, 2010] aboard LRO is studying water frost in the permanently shadowed regions (PSRs) at the lunar poles [*Gladstone et al.*, 2012], measuring the lunar night side surface using interplanetary Lyman-alpha and UV starlight as illumination sources, and investigating the lunar atmosphere [*Stern et al.,* 2012]. Water ice has a strong absorption edge in the far ultraviolet, near 165 nm [e.g., *Warren*, 1984]. This absorption is used to detect the presence of H_2O in the PSRs by measuring surface albedo inside the H_2O absorption and at wavelengths where H_2O does not absorb. On the dayside, the spectral slope of the surface albedo is found to increase over the H_2O absorption edge toward higher latitudes and early/late in the day [*Hendrix et al.*, 2012a], indicating increased abundances of surface frost in those locations. Abundances on the order of 1% by mass are measured using these techniques, and because the UV photons penetrate only the uppermost layers of the regolith, it is expected that the frost located is within a few microns of the surface.

The Moon has been observed extensively in the visible and shortwave-infrared wavelengths. Of particular interest in this spectral region is the 3-μm water ice absorption feature. A summary of the spectral measurements of polar regions of the Moon at 3 μm is provided in Table 6. Only three visible and shortwave-infrared instruments have observed the polar regions using reflected sunlight:

1. The Visual and Infrared Mapping Spectrometer (VIMS) on Cassini
2. The Moon Mineralogy Mapper (M^3) on Chandrayaan-1
3. The High-Resolution Instrument- Infrared (HRI-IR) on Deep Impact

A variety of other spectrometers have observed the Moon, but not at wavelengths that cover the 3-μm absorption band of adsorbed hydroxyl or water.

The Diviner thermal-infrared instrument [*Paige et al*., 2009] onboard LRO has also observed the entire surface of the Moon; however the limited spectral resolution and lack of spectral bands targeted to map any water ice absorption features in the far and thermal infrared has prevented any spectral identification of water ice so far using Diviner. However, Diviner has placed some of the most important fundamental constraints on the only locations where water ice (and other ices) will be stable on the lunar surface [*Paige et al*., 2010]. These measurements are fundamental to targeting future investigations of lunar ice.

In addition to optical spectroscopy methods, the Lunar Exploration Neutron Detector (LEND) has mapped the distribution of near surface (< ~1m) hydrogen and inferred water ice abundance, though the spatial scale of this instrument makes the interpretation challenging [*Mitrofanov et al*., 2010]. Furthermore, it is not possible to absolutely determine the physical nature of the hydrogen measured by LEND which may be in the form of a hydroxyl, hydrated mineral, or adsorbed to the surface.

The Mini-RF radar instrument on LRO [*Nozette et al*., 2009] measures total backscatter and polarization at wavelengths of 12.6 cm and 4.2 cm. Pure water ice deposits, such as the surfaces of the icy Galilean satellites, exhibit high radar albedo and circular polarization ratio > 1 [*Harmon et al*., 2001]. Although bistatic radar measurements from Clementine were interpreted as consistent with the presence of ice deposits near the south pole of the Moon [*Nozette et al*., 1996], these were later questioned [*Campbell et al*., 2006], and subsequent (monostatic) measurements by Mini-RF have not revealed clear evidence for substantial ice deposits. On the other hand, *Spudis et al*. [2013] interpret some craters with anomalous radar backscatter as being ice-filled. Upcoming bi-static radar measurements using Mini-RF and

Arecibo are expected to improve upon the Clementine results, and should clarify the situation.

An exciting recent discovery is that the lunar PSRs appear to have a higher 1064-nm albedo than illuminated terrain, based on backscatter measurements by LOLA [*Lucey et al*., 2014] (Section 4.7.1). Although it is difficult to quantify the abundance of putative surface ice using these measurements, the frost must be at least several wavelengths thick in order to be detectable. Unfortunately, albedo measurements at a single wavelength are not diagnostic of a water ice composition, and for the time being, must be interpreted in the context of other data, such as temperature.

4.6.1.3 Existing Laboratory Measurements

Reflectance and transmission properties of pure water ice have been studied in detail, from ultraviolet to microwave wavelengths [*Warren*, 1984; *Warren and Brandt*, 2008]. Much less has been done in the study of optical properties of ice/regolith mixtures.

Ultraviolet:
Hendrix et al. [2012b] provide a review of the UV laboratory measurements of ices. Water ice has been studied in the UV; however the temperature dependence of the spectral shape and crystallinity effects have not been well covered. Furthermore, spectra of H_2O ice in mixtures with lunar soil simulant have not been measured in the UV. Importantly, the spectral shape of OH has not been studied in the UV; it is therefore not understood whether the absorption measured by LAMP is completely due to H_2O or whether OH could play a role.

Shortwave-IR:
Water exhibits several strong, diagnostic vibrational bands in the shortwave-infrared, which have been studied extensively in the laboratory and through remote sensing, and radiative transfer models [*Warren*, 1982]. Observations and laboratory data suggest particle size plays an important role in the depth and shape of the near-IR bands. While some modeling has been done to quantify the effects of water ice contamination with dust, constrained somewhat by observations (primarily on Earth and Mars [e.g., *Salisbury et al*., 1994; *Langevin et al*., 2007]), only a few measurements have been made of the near-IR spectrum of ice/regolith mixtures under what could be described as lunar analog conditions [*Clark and Lucey*, 1984].

Thermal IR:
Thermal-infrared transmission of pure water ice of various crystallinities, in several thermal environments have been observed in the laboratory [*Moore and Hudson*, 1982; *Hudson et al*., 2013]. The mid-infrared water ice absorption features at 6 and 12 µm may be difficult to interpret due to mixing in a spectral region of strong silicate absorptions. Therefore, the far-infrared, where there is a fundamental water ice absorption feature at ~40-60µm, appears to be the best candidate thermal-infrared wavelength to characterize water ice abundance. This ~40-60µm ice feature varies in both position and shape based on the crystallinity (Figure 14), adding additional levers on the physical nature of surface water-ice.

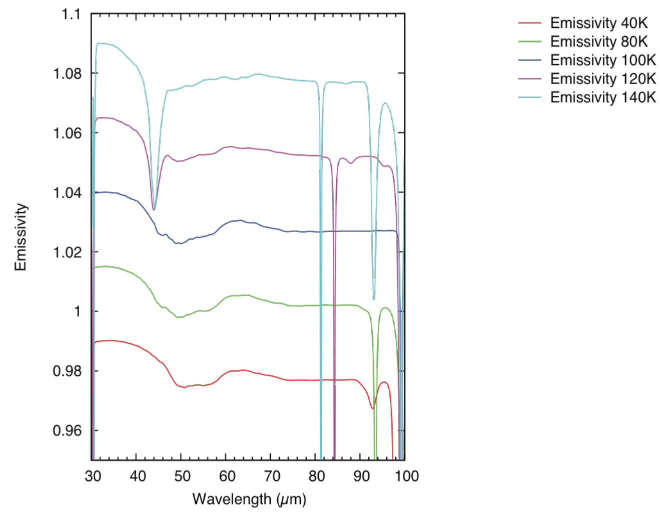

Fig 14: Water ice spectra from Hudson et al. [2013] which show changing crystallinity depending on the temperature at which the ice was deposited. The transmission spectra have been converted to emissivity assuming a particle size of 300 µm.

4.6.1.4 Model Results

Where laboratory measurements do not exist, numerical models can be run to provide some constraints on the nature of the ice and its detectability. The 3 µm band of water ice is the most sensitive one in the NIR spectral range. To determine the sensitivity of the instrument to the presence of water ice, we modeled various mixtures of a material "A" that simulates the lunar regolith with water ice, using *Pilorget et al*. [2013]. Material A could be basalt, basaltic glass, or a material whose properties were directly derived from Apollo samples spectra. Its grain size distribution follows an r^{-3} power law to mimic the one of the lunar regolith. This material is then mixed with water ice to simulate intimate mixtures. Water ice grain size is set to 20 µm, but other sizes were also tested. The thermal contribution was also added for different scenarios.

Spectral modeling shows the presence of a local maximum around 3.15 µm, which can be used to discriminate the water ice from OH bearing materials (Fig 15, left). Assuming that the instrument will be able to detect 5% absorption features on 10% albedo surfaces, modeling results suggest that water ice fractions of ~10% (in

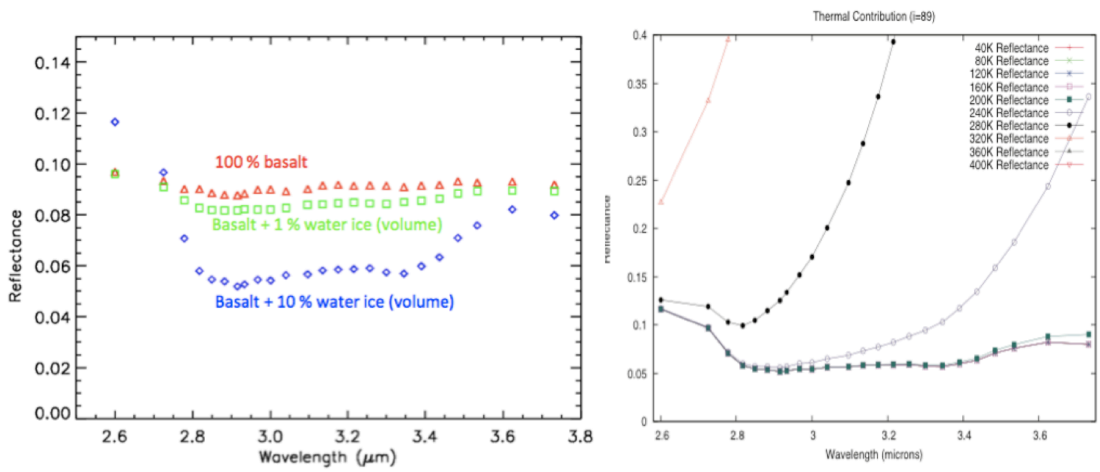

Fig 15: (left) NIR reflectance spectrum of basalt/water ice intimate mixtures modeled with Pilorget et al. [2013]. Basalt grains follow a r^{-3} power law granulometric distribution between 20 and 400 microns and water ice grain size is set at 20 microns. (right) NIR reflectance spectrum of a 90% basalt-10% water ice intimate mixture with the addition of the thermal contribution, for different temperatures.

volume, thus ~4% in mass) could be detected and discriminated from OH-bearing materials. Assuming a capability to detect 1% absorption features, the sensitivity to water ice could increase to ~1% (in volume, thus ~0.4% in mass). In case of larger water ice grains, the sensitivity would also tend to improve. Importantly, the thermal contribution does not affect significantly the spectra for temperatures below 200 K, which is much above the expected temperature in the craters, and could thus be neglected (Fig 15, right).

Missing laboratory experiments:

While nearly every spectroscopic method presented here has a suite of laboratory measurements designed to characterize ice, primarily for icy moons and the terrestrial cryosphere, few studies have been conducted to date which are designed to characterize the behavior of small amounts of water ice in contact with a lunar regolith in a lunar environment. Laboratory studies across the shortwave- and thermal infrared that measure several ice/regolith mixtures with varying fractions of ice and different thermal conditions, including warm deposition, cold deposition, and variations in thermal history, would greatly improve the estimates of detectability from orbit and constrain existing numerical models. The differing thermal environments would help simulate variable levels of crystallinity and the respective change in spectral shape, providing important constraints on the thermal history the lunar ices have experienced and the potential formation mechanisms.

Table 5. Observations of ice from the moon and laboratory, which illustrates areas that require future examination.

Wavelength	Current state of PSR Coverage	Ice Discrimination	Current Laboratory Observations	Missing Laboratory Observations
UV	YES	Good	Limited – pure H_2O ice only	1) H_2O ice/regolith mixtures 2) Crystallinity variations 3) Shape of OH vs. H_2O bands
Shortwave-IR	NO – Requires illumination	Good	Limited – pure H_2O ice only	1) H_2O ice/regolith mixtures 2) Crystallinity variations
Thermal-IR	YES – Temperature only	Unknown	Limited – pure H_2O ice only	1) H_2O ice/regolith mixtures 2) Crystallinity variations 3) Thin Films
Radar	Some – Limited bi-static radar	Large blocks only	Terrestrial cryosphere studies	1) Characterize/calibrate rock/ice relationship for bi-static radar measurements

Table 6: Summary of shortwave-infrared observations of the moon

	VIMS/Cassini	M^3/Chandrayaan-1	HRI-IR/Deep impact
Type of observation	1 Flyby, Quarter Moon, South Pole observed	Polar orbit, 100-200km altitude [*Boardman et al.*, 2011]	3 Flybys Sub-spacecraft latitude: 1) 4S (small equatorial area), 2) 75N and 3) 77 N (polar view for both) [*Sunshine et al.*, 2009]
Number of observations	11 full/2 partial images [*Clark*, 2009]	95% of the Southern polar region 90% of the Northern polar region	3
Spectral range (μm)	0.3505 – 5.12 0.3505 – 3.4 [*Clark*, 2009]	0.43 – 3.0 [*Green et al.*, 2011]	1.05 – 4.8 [*Hampton et al.*, 2005] 1.05 – 4.5 [*Sunshine et al.*, 2009]
Spectral resolution at 3 μm (λ/Δλ)	127	75	220
Spatial resolution (m/pixel)	175000 [*Clark*, 2009]	140 - 280	1) 10000, 2) 78800, 3) 58800 (3) [*Sunshine et al.*, 2009]
Observation of adsorbed OH or H_2O	[*Clark*, 2009]	[*Pieters et al.*, 2009; *McCord et al.*, 2011; *Cheek et al.*, 2011]	[*Sunshine et al.*, 2009]
Thermal emission correction	[*Clark et al.*, 1979]	Incomplete for spectra of areas that have hydrated components [*Clark et al.*, 1979, 2001]	[*Groussin et al.*, 2007]

4.6.2 Trajectory and Navigation of Small Spacecraft

The gravitational dynamics of the Moon is unique in the Solar System. The Earth-Moon 3 Body System has the largest mass ratio M_{moon}/M_{earth} of any 3 Body System in the Solar System. This is further complicated by the Sun-Earth 3 Body System because the range of energy to escape the Earth overlaps the energy to escape the Moon. And in this energy range is where chaotic dynamics dominate. This is what provides the ultra-low energy orbits used by missions like Genesis, Grail, and Artemis. But the chaos can also wreak havoc on loose orbits around the Moon, particularly where resonances overlap. For larger spacecraft with more powerful propulsion systems, one can quickly pass through the resonances or avoid them all together. But with SmallSats and their less capable propulsion systems (e.g. ion engines or solar sails), a difficult passage through the resonances is inescapable. One of the physical manifestations of the problem is that the perilune of the orbit will vary wildly from orbit to orbit which can easily crash the spacecraft during a close perilune passage.

However, the situation is by no means hopeless. In fact, the most dangerous resonances for the Lunar Flashlight mission [*Hayne et al.*, 2013b] (those we have discovered so far) seem to be close to the 1-1 resonance which has a period of ~28 days. Since the passage through perilune is the point of danger, which occurs only once per orbit, we actually have a long time to design, prepare for and perform the station keeping maneuvers to avoid crashing at the perilune passage. We must note here that the passage is not through a single resonance, but rather through a cluster of overlapping resonances starting from the 1-1 resonance that creates this dangerous chaotic regime. When the orbit becomes much smaller (period < 1 day), the gravitational effects of the Sun and the Earth become greatly reduced and these resonance effects are greatly diminished.

The actual maneuver size will likely be very small since we can exploit the chaos for the control. What is not known at the present is the dynamical structure of these chaotic regions and the station keeping strategy for controlling the chaos. Work is needed in these two areas in order to solve this problem.

The passage through overlapping chaotic resonances is a problem faced by many missions that need to capture into orbit around a body using resonant flybys. Missions to the Jovian and Saturnian moons like Europa, Ganymede or Titan must all face this problem. Thus the work proposed here will be applicable to these other missions as well. Although each system has its own resonance structures so the control strategy must be adjusted and custom designed for each mission's requirements. However, the general theory and strategy developed for controlling resonance passage at the Moon will contribute to these other missions.

4.7 Mission and Instrument Concepts

Here we describe several mission concepts, which could be capable of making the key measurements presented in Section 4.1. This set of concepts is not intended to be comprehensive, but represents several of the most promising candidates studied. We detail the highest-priority concepts in each of the following three categories:

- **Orbiting spacecraft**: *active* multispectral reflectance measurements in the shortwave-infrared or passive multispectral emission measurements in the thermal-infrared, for definitive detection and mapping of water and other volatiles within several micrometers of the surface
- **Penetrator probes**: targeted, instrumented probes capable of detecting ices and quantifying their depth distribution at >3 distinct sites using neutron spectroscopy, mass spectroscopy, and/or tunable laser spectroscopy
- **Impactor probes**: targeted, well-characterized impacts observed from a separate Moon- or Earth-based platform in the ultraviolet to microwave spectral range to detect ice and vapor released at >3 distinct sites

4.7.1 Orbital Spectroscopy

No orbital remote sensing method has been flown or proposed previously that is unambiguously sensitive to the abundance of the water molecule in extensive regions of permanent shadow, which can be obtained at high resolution, and also on the sunlit Moon. It is possible that an extremely sensitive shortwave-IR spectrometer could measure 3-µm spectra in portions of polar shadow using stray light from nearby illuminated regions, but this excludes large flat-floored craters, and must contend with the fact that the illumination source – sunlight reflected from the lunar walls – is itself contaminated by ubiquitous 3-µm features in the illuminated polar lunar material.

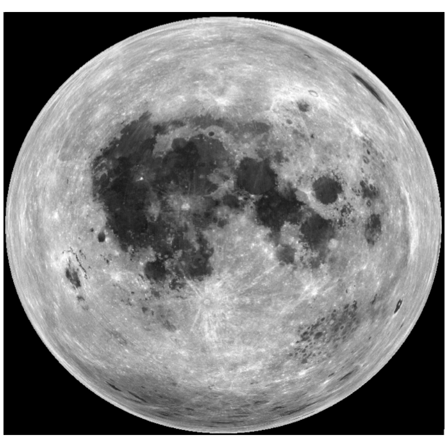

Fig. 16: Active laser imaging has been demonstrated. Image of the Moon from LOLA produced from the LOLA return pulse intensity. Lambert projection.

One possible solution to the problem of water detection on the Moon is to use an multispectral shortwave-IR coupled with an active illumination source, such as a solar reflector. For example, Lunar Flashlight, a CubeSat mission concept being studied by AES, would utilize a solar sail to shine reflected sunlight into the lunar PSRs [*Hayne et al.*, 2013b].

Another possible solution is active laser spectroscopic imaging in the 3-µm spectral region. The Lunar Orbiting Laser Altimeter (LOLA) [*Zuber et al.*, 2012], and before it, the Mars Orbiting Laser Altimeter [*Neumann et al.*, 2003], proved that quality planetary surface reflectance measurements could be obtained by measuring the strength of the reflectance laser return, and images can be constructed by gridding these returns. Figure 16 shows a global image of the Moon derived entirely from the LOLA laser return signal, and Figure 17 shows a close-up of the immediate lunar south pole featured by *Zuber et al*. [2012]. This technique is also powerful for measurements of water on the illuminated portion of the Moon because the laser reflectance measurements are not contaminated by reflected solar illumination or by lunar thermal emission; few photons are present in the 10-20 nm integration times of the APD detectors used by planetary LIDAR instruments; therefore, the measurement is essentially pure reflectance. Similar images in key spectral bands for water would enable mapping of water and related species moon wide, and in regions of permanent shadow.

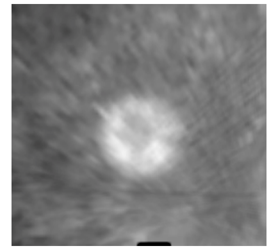

Figure 17: Image of permanently shadowed Shackleton crater obtained by LOLA. From Zuber et al. [2012].

For both types of active shortwave-infrared instruments, the suggested spectral range corresponds to the minima of all the major water species (Figure 18), and also includes the C-H feature at 3.4 microns for organic detection. The width of the spectral lines is more than adequate to sample the relevant spectra, and a small number of bands would allow discrimination of these species for example at 2.65 (for reference), 2.8, 2.9 and 3.1 µm. Wavelengths beyond 3.1 µm provide more diagnostic information regarding the presence of ice (Figure 18), and give insight into the presence of organics through detection of C-H stretches near 3.4 µm. This wavelength region also can serve as a second continuum point as lunar space weathering likely causes slopes that could be misinterpreted as spectral features with more limited coverage.

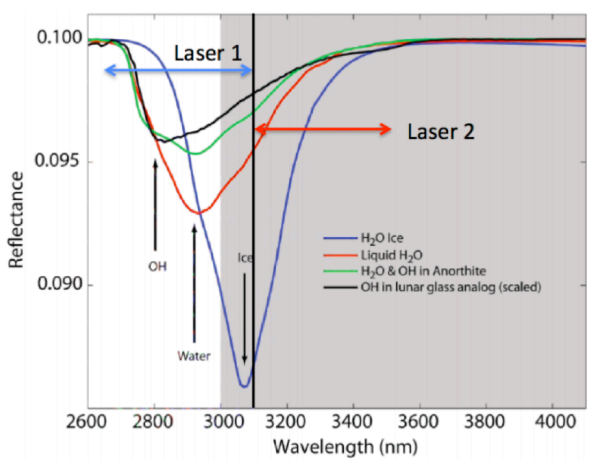

Figure 18: Spectra of water-related phases from Pieters et al. 2009 with two laser ranges that could be used in a flight instrument. Laser 1 would sample the continuum and the minima of the major water species. Laser 2 would provide additional information on ice, organics and a second continuum wavelength.

Based on preliminary calculations, the sensitivity of these types of instruments could be better than 1% of the reflectance. The 3-µm region is extremely sensitive to the presence of water, so the detection limits extend to very low abundances. A 10 nm water film on a silicate substrate has a 3-µm band depth much more than 1% (Figure 19). In the form of ice grains intimately mixed with the regolith, a 1% band depth corresponds to an ice abundance of 1 part in 500 (single scattering albedo from

Hansen [2009], calculation using *Hapke* [1993]) (Figure 14). *Klima et al.* [2013] showed that 5% band depth corresponded to 80 ppm (+/- 40) bound water, so the laser instrument's detection limit in the special case of adsorbed water would be better than 20 ppm with a 1% 3-μm feature depth.

A third instrument concept would utilize water ice absorption bands in the thermal-infrared, which are sensitive to both the abundance and physical nature of water ice (section 4.4.4). Thermal-infrared techniques do not require solar illumination and LRO's Diviner Lunar Radiometer has already demonstrated adequate temperature sensitivity in permanently shadowed regions. Although this is potentially a very powerful concept, the strength of water ice absorptions in regolith mixtures and the shape of bands as a function of crystallinity are very poorly constrained. Therefore, additional laboratory and modeling studies are required before the capabilities of this type of instrument can be evaluated.

Adequate spatial resolution is another important constraint for orbital spectroscopy techniques. In the case of the PSRs, requirements would be scaled to the geologic features of interest. Figure 17 shows the floor of the 20 km south polar crater Shackleton using 1064 nm active reflectance data from LOLA. The floor of this crater is about 5 km in diameter, so ~0.1 km resolution would easily resolve the floor of this candidate ice location, and provide many-pixel resolution on the walls. We advocate investment in technology development to push these promising new types of instruments toward flight readiness.

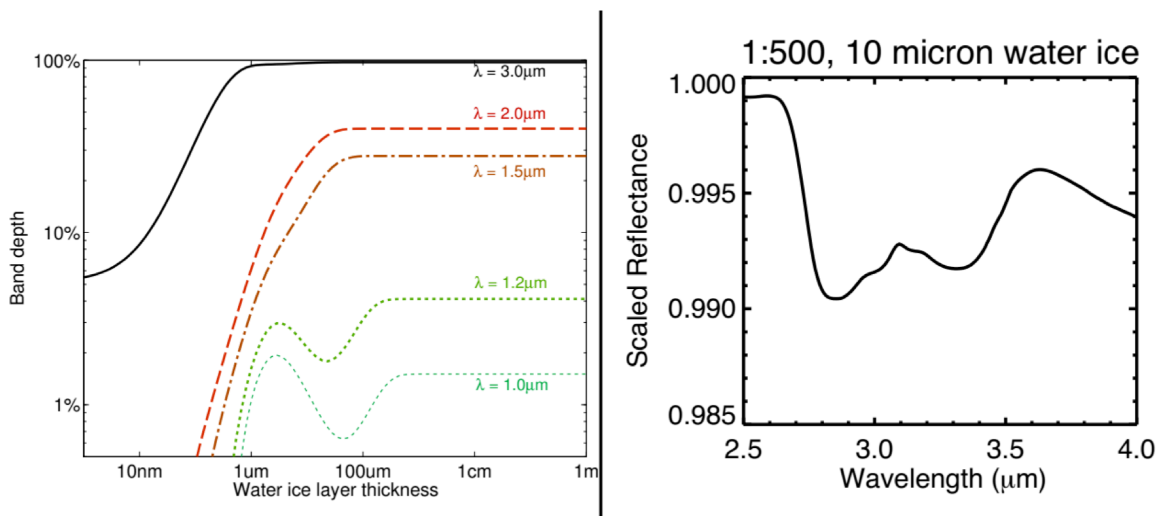

Figure 19: Left, depth of various bands vs. water film thickness on a silicate substrate. Note at 3 μm (black line) band depths are well above the detection limit of 1% reflectance for a thickness of 10 nm. Right, scaled model spectrum of 0.2 wt% 10-μm ice grains mixed with a plagioclase substrate showing a 1% band depth at 3 μm.

4.7.2 Penetrator Probes

Penetrators are a class of instrumented probes capable of surviving high-speed impact into planetary bodies for the purpose of making scientific measurements at some depth beneath the surface. Although penetrator technology has its origins in military applications, many different studies and proposals have advocated its use for planetary science and exploration [*Lorenz*, 2011]. The Moon is both a technically compelling and challenging target for penetrators, due to its proximity to Earth and its ubiquitous regolith, yet its absence of an atmosphere for stabilization. As we discuss here, penetrators are also highly suitable for making measurements to address the abundance, distribution, and origins of lunar ice.

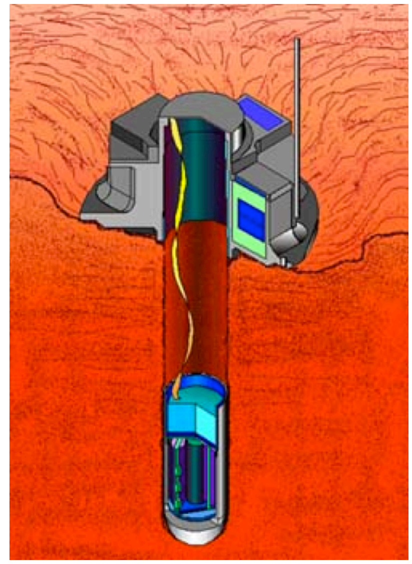

Figure 20: Illustration of the Deep Space 2 penetrator probe, which was a secondary payload on the Mars Polar Lander Mission. (Credit: NASA)

Although there have been no successful planetary penetrator missions as of yet, extensive development has brought the technology to a high readiness level. The Deep-Space-2 (DS-2) penetrator probes, developed by JPL, were built and flown on the ill-fated Mars Polar Lander mission (Fig. 20) [*Smrekar et al*., 1999]. Perhaps the best-developed lunar concept, the Japanese Lunar-A mission included at least one penetrator equipped with seismometers and heat flow probes, but unfortunately this technically mature mission was canceled after an investment of ~$132M [*Normile*, 2007]. *Lorenz* (2011) provides a comprehensive history and technical overview of these and other planetary penetrators.

Instrument Requirements

Lacking an atmosphere for deceleration and stabilization, lunar penetrators must tolerate high velocity impacts typically dictated by a "stop and drop" method of de-orbiting using onboard propulsion. Drop heights < 30 km yield impact velocities < 300 m/s, which is a common requirement if instruments are to experience < 10,000 g loads [*Lorenz*, 2011]. Volume, mass, and power are typically secondary requirements that may preclude some instruments. Typical cylindrical penetrators are ~1 m in length and 2–120 kg, accommodating a small payload that consumes ~1 W power. A major consideration is battery life, which may be < 12 hr without the aid of an RTG [*Mosher and Lucey*, 2006]. Therefore, instrument integration time must be taken into account. Burial depths of ~1–2 m can be expected, with instrumentation perhaps distributed along the lower half of this distance.

Application to Science Goals

For the purposes of lunar ice detection and mapping, penetrators offer a number of advantages over other in-situ platforms and orbital spacecraft:

- Direct in-situ measurements at a range of depths in the subsurface
- Good thermal and mechanical contact with the regolith
- Point-like measurements at a highly localized scale
- Possibility of probing multiple targeted sites with several penetrators

In addition to these scientific advantages, penetrators are seen as relatively low-mass, low-cost options for acquiring in-situ data. Among the possible penetrator payloads, we studied the potential of several instruments for ice detection:

- Neutron detectors
- Mass spectrometers (Mass-spec)
- Tunable laser spectrometers (TLS)
- Temperature/heat flow probes
- Electrical conductivity probes
- Dielectric spectrometers

Several other instruments were discussed, but not studied in detail (e.g. Alpha-proton X-ray spectrometers, microwave spectrometers, radar). The first-order requirement is that the technique be able to unambiguously differentiate water ice from dry regolith at levels < 0.5wt% (see Section 4.3). Secondly, a major advantage of penetrators is their ability to sample discrete depths, and therefore the instrument must be capable of such measurements. Third, determining isotope ratios of evolved volatiles could address questions of their origins, which is a major science driver of this study.

Given the above considerations, temperature and heat flow probes are inadequate due to their expected measurement uncertainty for H_2O content and ambiguity in determining the water ice depth profile. Electrical conductivity probes and dielectric spectrometers may meet the measurement sensitivity requirements, but probably suffer from the same issues in measuring discrete depths.

Neutron detectors are capable of measuring hydrogen abundance (regardless of its molecular state) at extremely low abundances [*Feldman et al.*, 2000]. Discretely spaced neutron detectors along the length of the penetrator could also recover the depth profile of hydrogen at the required sensitivity. The major weakness of neutron detectors is their inability to determine the chemical state of H atoms, and therefore other information would be required to assess the relationship to regolith water content.

Mass spectrometers and TLS offer similar opportunities for measuring diverse volatiles at extremely low abundances, and to determine their isotopic composition.

Sample ingestion systems for penetrators have been developed and demonstrated, and mass spectrometers have been shown to survive > 1,000 g loads and remain fully functional [D. Lawrence, *personal comm.*]. TLS is an extremely durable and compact option, with precision possibly far exceeding mass-spec. The major potential shortcoming for this application is the necessity for multiple instruments and sample acquisition systems along the length of the probe, which will drive up mass, complexity and cost.

Based on these and other considerations, we recommend a penetrator payload consisting of both:

- Either a mass-spectrometer or TLS and sample acquisition system (probably near the nose of the probe), and
- Several (> 2) neutron detectors evenly spaced along the interior body of the probe

This payload has the ability to meet all of the above science goals, and includes high TRL hardware already tested on penetrators. Finally, in order to fully satisfy our top-level science goal, multiple penetrators must be deployed to surfaces exhibiting diverse thermal environments.

4.7.3 Impactors

Remote sensing observations are limited to the upper microns to decimeters of the surface depending on wavelength, and sometimes cannot uniquely determine the bulk composition. Mechanical excavation using drills, shovels, or similar techniques can provide stratigraphic recovery of material from depth, but requires an excavator on the surface, thereby increasing cost and complexity considerably. Impacts, however, serve as an alternative process of "kinetic excavation," and are the cheapest and easiest way to access subsurface material on planetary bodies (Fig. 21). During a hypervelocity (in excess of the sound speed) impact on a planetary body, strong shockwaves and subsequent rarefaction waves set material in motion, excavating and ejecting a portion of the target up and out of the crater to expose fresh material from depth. While fresh ejecta patterns and steep slopes of craters

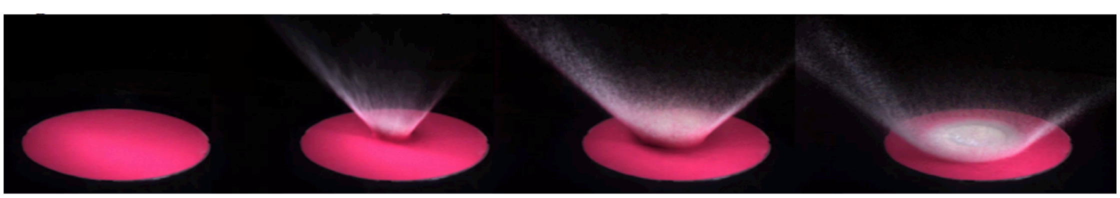

Figure 21: Time series of a laboratory impact experiment. A 6.35mm Al projectile launched at 60° from horizontal into a sand target. Downrange is to the left. The sand, nominally tan, was overlaid with a thin lamina of darker red sand to highlight the inversion of stratigraphy and excavation of material from depth. Images are taken at just before impact, ~35msec, ~70msec (end of crater growth), and ~140msec. Figure from: Hermalyn and Schultz [2012]

from natural impacts have long been used to infer properties of the subsurface, recent artificial impacts have demonstrated the utility in observing and measuring the ejecta during the impact event: the Deep Impact (DI) mission (e.g., *A'Hearn et al*. [2005], *Schultz et al.* [2007]), which excavated material from the subsurface of comet 9P/Tempel-1, and the LCROSS mission (e.g., *Colaprete et al*. [2010], *Schultz et al*. [2010]), which used the upper stage of a rocket as a kinetic impactor.

Among recent investigations related to lunar volatiles, the LCROSS impactor mission ranks as the most direct. In this experiment, the upper stage of the launch vehicle was impacted into the persistently shadowed portion of the south polar crater Cabeus. The impact lofted subsurface regolith and volatiles into sunlight, where they were observed by a shepherding spacecraft. Although the detection of water in this ejecta material (~2-7wt%) has been made with relative certainty, several remaining questions prompted us to study the potential for additional impactor missions:

- *How is the detected ice distributed vertically and horizontally at the LCROSS impact site?*
- *Is this site representative (in terms of volatile content) of similar polar cold traps?*
- *To what extent does impactor contamination contribute to the observed volatiles?*
- *How can smaller kinetic excavators (CubeSat-sized) be effectively used to sample other regions of the lunar subsurface?*

Impactors are advantageous in that they do not require a landing system, yet are capable of providing *in situ* extraction of material from the subsurface. The kinetic excavation is not the measurement itself, but is considered more as a mechanism Successful measurement of these lofted species requires simultaneous observation by at least one other asset, either at the Moon or Earth, and (depending on the detection technique), illumination by the sun. Therefore, understanding the behavior and mass-velocity distribution of the ejected material is of significant import to mission success.

Previous experience with artificial impacts (ranging from Apollo S-IVB stages to the LCROSS centaur upper stage) has shown that the geometry and failure mode of the impactor plays a significant role in shaping the evolution of the ejecta. For example, the low density Centaur impactor for LCROSS created a high-angle plume that greatly enhanced the lofted volatiles in the spectrometers' fields of view versus traditional "sphere" impactors for several minutes after the impact (as was predicted from pre-impact testing results at the AVGR; [*Schultz et al*., 2006, *Hermalyn et al*., 2009]). CubeSat or nanosat-deployed impactors are expected to have similar non-standard ejecta patterns that can be optimized via "tuned" impactor geometry to enhance possible detection of volatiles. In addition to quantifying volatile abundance, it may also be possible to determine the isotopic composition of volatile species, lending insight into their origins.

Here we describe two possible missions capable of making the key measurements. It is noted that to maximize lofted material, most impact missions on the Moon are tuned to impact at near vertical incidence (90°) from Earth escape (or similar, such as L2) orbits (~2.5km/s). Impacts from lunar orbit are possible, but will significantly reduce the amount of lofted material due to their grazing impact angles (<10°) and lower speed (~1.6km/s).

Impactor and Follower with Spectrometer

In this mission concept, at least one impactor probe is paired with one or more shepherding spacecraft carrying spectrometers to determine volatile content in the excavated ejecta cloud. Several instruments could be used, including infrared/visible spectrometers (potentially with active illumination to permit measurement beneath the sunlight horizon) and/or a microwave spectrometer capable of discriminating among isotopologues of H_2O. As described in Section 4.4.6, such an instrument can be made relatively compact and requires no illumination source.

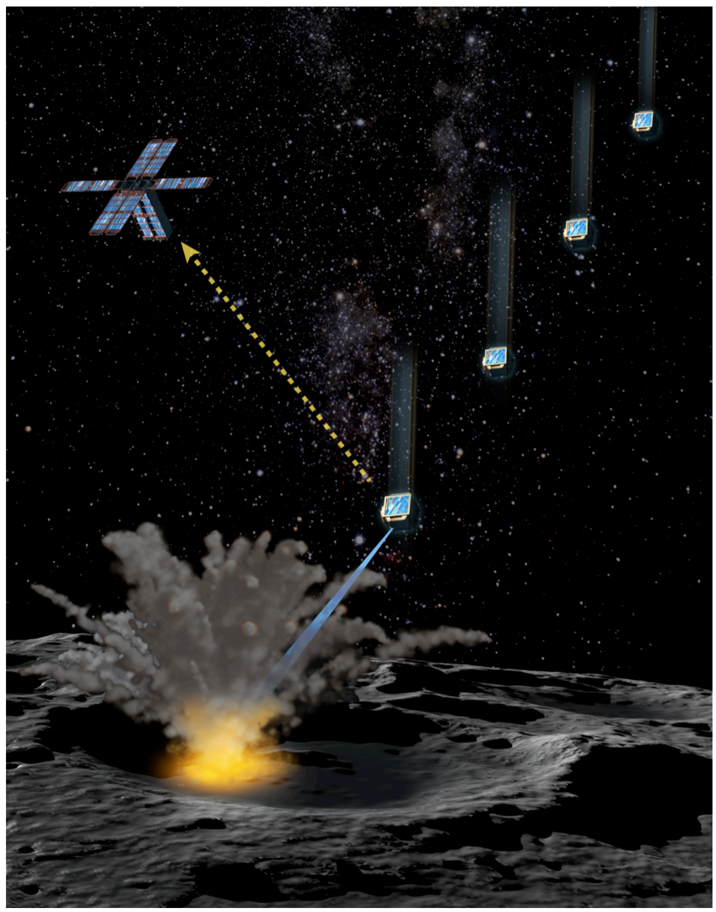

Figure 22: Artist's conception of a multiple impactor/chaser CubeSat mission concept for detecting lunar volatiles. Either a relay satellite, or direct-to-Earth communications could be utilized to transmit observational data from impacts at multiple locations.

Multiple impact sites should be targeted, to sample the full range of polar thermal environments, including a sunlit region as a control on the experiment. This could be accomplished by a "string of pearls" sequence of impactors (Fig. 22), where each subsequent impactor observes the previous and relays its data to a "mother ship" relay satellite, or direct to Earth.

Impactor and Lander or Chaser with Gas-phase Sample Chamber

This scenario includes at least one impactor and either a "chaser" spacecraft or lander carrying a gas-phase sample chamber capable of detecting and identifying isotopologues of water and other volatile species. Similar to the spectrometer measurements described above, the mission design should lead to sampling (either targeted or stochastic) of multiple locations in different thermal environments.

Feasibility

An initial feasibility study was conducted in conjunction with the NASA Ames Mission Design Center to assess whether CubeSat-sized impactors were capable of lofting sufficient material to be realistically measured and characterized in such scenarios (Fig. 23). Building on prior experience from LCROSS and several NASA PGG-funded projects to understand fundamental cratering processes, a preliminary assessment of the mass delivered above a given height as a function of time for several CubeSat impactor sizes was carried out. Since many regions of interest in the polar areas of the moon are in deep shadow (for example, the region in Cabeus that LCROSS impacted had a solar horizon of 833m), this is a strong constraint on planning. Removal of this constraint –through active illumination, careful site selection, and/or measurement techniques that do not require illumination- would significantly enhance the efficacy of small impactors to loft material in measureable quantities.

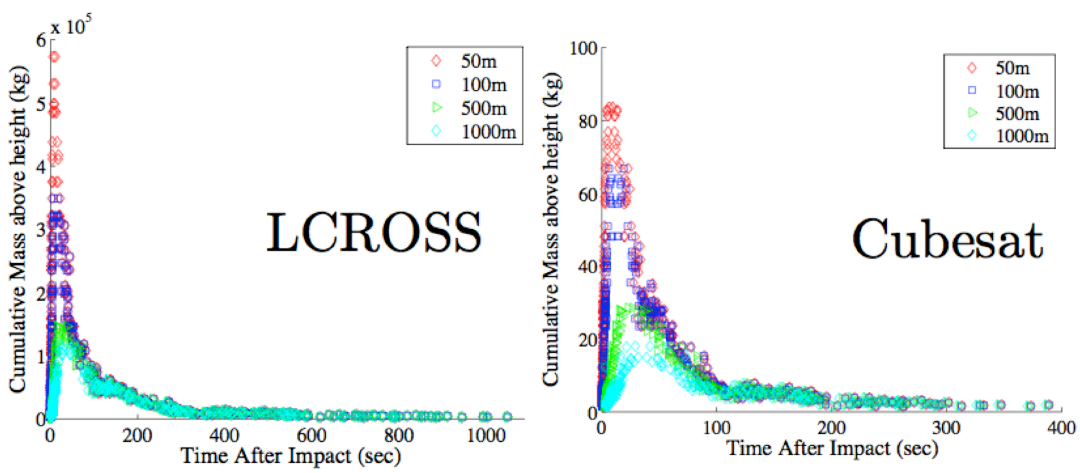

Figure 23: Comparison of cumulative mass lofted above 50, 100, 500, and 1000 m for LCROSS (left) and a CubeSat (right).

4.7.4 Mission Concept Prioritization

Each of the proposed mission concepts could satisfy the key measurement requirement of quantifying ice at the 0.5wt% level within the top few meters of soil, at multiple (diverse) sites. Based on the perceived scientific merit of each concept, we prioritized them according to the flowchart below (Fig. 24). Although penetrator probes may have the greatest scientific potential, we prioritize microwave sounding of multiple impact plumes, due to the perceived combination of strong science return and low cost and risk.

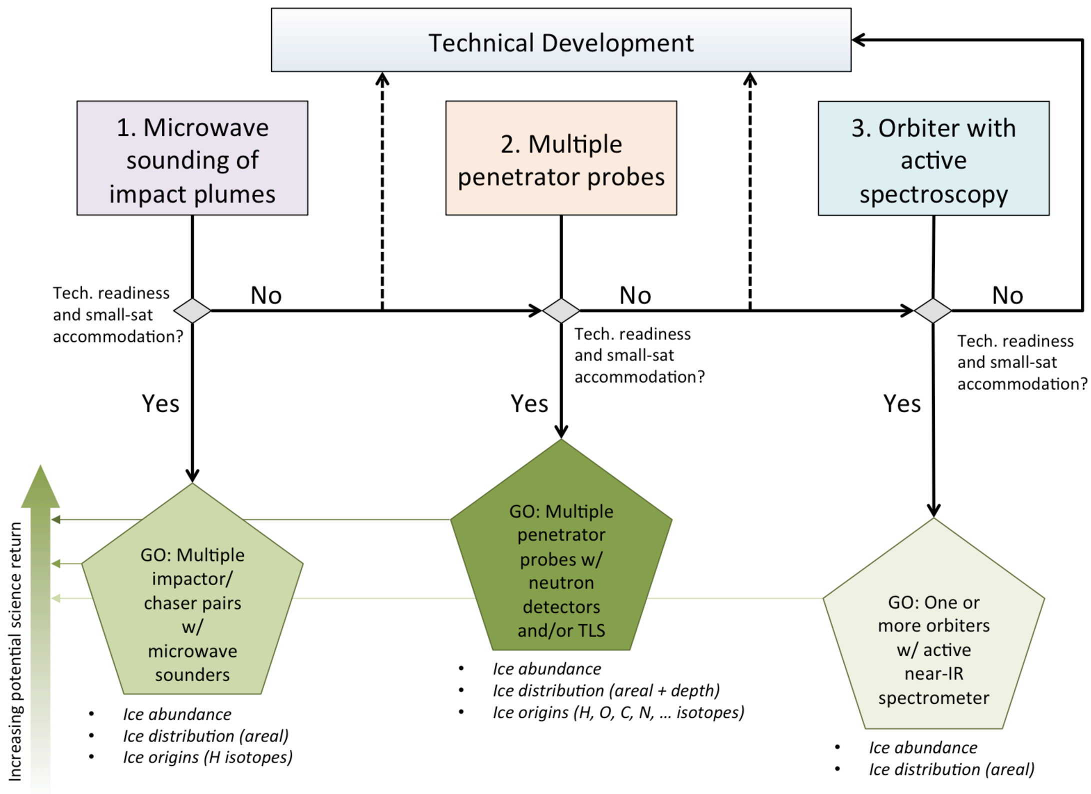

Figure 24: Small-sat lunar ice detection missions flowchart for technical development

4.8 Small Satellite Technology

4.8.1 Current State of the Art and Challenges

Small satellite systems are devoted to an incredible variety of missions from bus to component testing, to complete science missions (including astrobiology, space weather and Earth systems research). CubeSat developers, in particular have demonstrated the versatility and capability of the CubeSat using payload systems based on miniaturized electronics, micro-electromechanical systems (MEMS technologies) and innovations in sensor and microprocessor and microcontroller systems. To date, CubeSat missions have focused on the following applications:

- *Technology Demonstration*
- *Earth Remote Sensing*
- *Ionospheric and Auroral Research*
- *Effects of the Space Environment on Biological Systems (Astrobiology)*
- *Radiation Affects on Space Technologies*
- *Astrophysics*

An assessment of the current state of CubeSat technology facilitates extrapolation toward a prediction of future trends and technological advancements. Recently, the small satellite community has seen dramatic improvement in the performance and capabilities of subsystems, including higher bus power, deployable systems, improved processor architecture, more robust and radiation tolerant components, and higher bandwidth/throughput communication systems. These systems have tremendously enhanced the capabilities of CubeSats as evidenced by the number of commercial aerospace ventures now flying them.

Future advances, particularly in the areas of flight dynamics, advanced power, processor systems, and propulsion will facilitate a wide variety of science and commercial payloads. These advances are driven by the current revolution in micro-electronics, especially in the area of MEMS devices. Passive spacecraft stabilization systems have been refined, and low-cost commercial active stabilization and orientation systems relying on momentum wheels and magneto-torquers are now available. Horizon sensors, Sun sensors and star trackers are also now becoming commercially available. MEMS-based and other propulsion systems are being developed that will be used for spacecraft orientation and orbit adjustment.

These technologies are beginning to facilitate experiments in optical and IR imaging, spectroscopy, astrophysics (i.e., the study of highly energetic astronomical phenomena) and space physics (i.e., the study of aurora, magnetic fields, radiation belts, and the plasma-electrical environment of the Earth-Sun system). Studies of the Earth in regard to its natural resources and aspects of climate change are also facilitated by these advancements.

Several key enabling technologies are facilitating this transition of small satellites from technology demonstration to science platforms. These key technologies include: high Isp propulsion systems, low cost radiation tolerant electronics, miniaturized attitude determination systems, significant on-orbit processing capability, and high bandwidth communication systems. Other technologies take a supporting role including 3-D printing in non-conventional materials, rigidizable and inflatable structures, and the ability to accurately model space radiation effects.

Propulsion Technologies

An important next step in the evolution of small spacecraft is the implementation of capable propulsion systems, as most of the really interesting applications require some level of mobility. Applications that require this mobility include formation flying of multiple CubeSats, fractionated satellites, atmospheric drag make-up, and low cost missions to the Moon, asteroids and planets of the Solar System. Numerous space missions are now being developed that have cold gas and miniaturized systems similar to those used in larger satellites. Other more exotic systems are being developed for use on smallsats and even CubeSats that will feature unique and innovative propulsion systems. These developments are being supported in part by the fact that larger, more expensive satellite missions cannot afford the risk associated with these unconventional propulsion systems being tested by smallsat developers.

An example of innovative propulsion systems for CubeSats includes cold/warm gas propulsion utilizing MEMS-based engine nozzles and exotic bi-propellant systems.

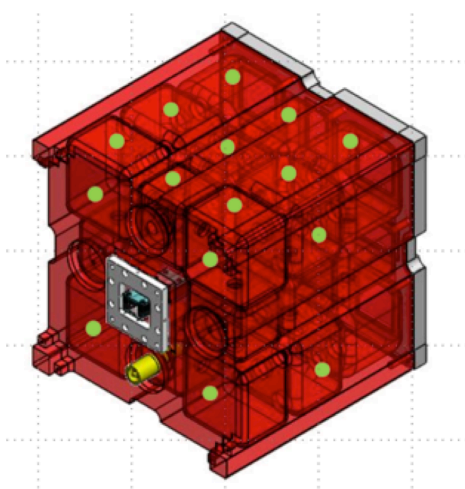

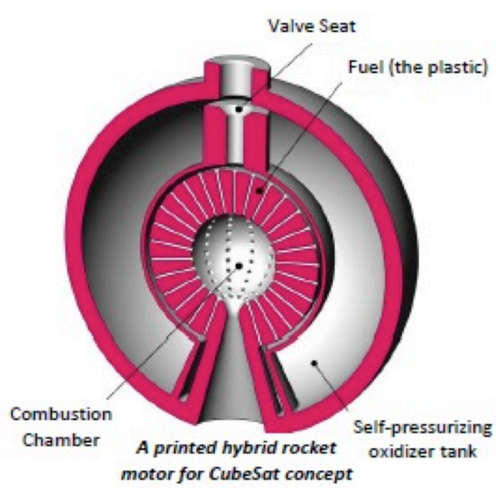

Figure 25: (Left) Heated Freon gas propulsion (Courtesy of Adam Haung, U. Arkansas), (Right) 3D-printed integrated propulsion (Courtesy of Matthew Dushku and the Experimental Propulsion Lab)

Figure 25 shows a 3D printed complex propulsion system being used on a 2U CubeSat for orbit altitude augmentation using a heated Freon gas.[2] Figure 25 also shows a 3D printed bi-propellant system (Additive Manufactured Propulsion System) that uses part of the structure as one of the burned components and can also be used in cold gas mode.[3] Using this 3D printing technology, these structures are very inexpensive to manufacture and can have very complex shapes. As shown in Figure 26, part of the construction material can be used as one of the burned components of the hybrid motor combustion.[4]

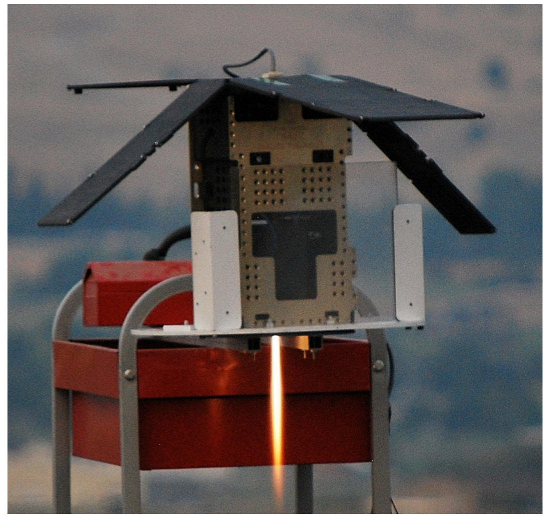

Figure 26: 6U Cubesat Chassis with 1.5U AMPS-H motor, 2012 (Courtesy of Matthew Dushku and Experimental Propulsion Lab)

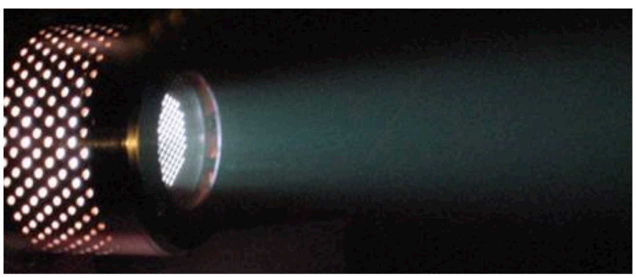

Figure 27: Busek BRFIT-3 3cm RF Thruster Operating at 100W Total Power. Credit: Busek Co., Inc.

Other CubeSat propulsion systems under development take a more conventional approach, but with a twist to accommodate the CubeSat form factor. Several groups are working on miniature ion propulsion systems that are ready for implementation on CubeSat systems. In 2013 July, NASA selected three developers of "electrospray" propulsion for support under its Game Changing Development program: Busek, JPL, and MIT [*Rink*, 2013]. One example is an MIT propulsion system works slightly differently than a conventional ion drive. In a typical ion engine, electricity ionizes a gaseous or liquid propellant as it enters the thruster, and the positive ions are accelerated between grids having a high voltage difference. Electrons are accelerated separately and injected into the ion exhaust stream to prevent space charge buildup. In the MIT engine design, the propellant is pre-charged on the ground and encapsulated in

---

[2] The RAMPART CUBESAT (Rapid prototyped MEMS Propulsion and Radiation Test CUBEflow-SATellite) incorporates a MEMS-based cold gas thruster. The RAMPART team includes Gilbert Moore (Project Starshine), Walter Holemans (Planetary Systems Corporation), Adam Huang, John Lee and Matthew McMullen (Department of Mechanical Engineering, The University of Arkansas), Jim White (Colorado Satellite Services), Robert Twiggs, Benjamin Malphrus and Nathan Fite (Space Science Center, Morehead State University), David Klumpar, Ehson Mosleh and Keith Mashburn, (Space Science and Engineering Laboratory, Montana State University), David Wilt and James Lyke (U.S. Air Force Research Laboratory/Space Vehicles Directorate), Stewart Davis (CRP USA, LLC), Wes Bradley (Analytical Graphics, Inc.), 2Lt. Thomas Chiasson (USAF), Jay Heberle (Universal Space Network) and Pat Patterson (Space Dynamics Laboratory)

[3] Dusku, Matthew and Mueller, P. "Aditively Manufactured Propulsion System," 26th Annual AIA A/USU Conference on Small Satellites.

[4] Manufactured by Planetary Systems and tested at the AIAA/USU Small Satellite Conference, August 2010.

small needle-like structures. When an electric charge passes through the needles, the propellant is accelerated in the focused electric field and expelled. Since each needle is effectively its own engine, the entire system is modular and customizable.[5] Another example is a series of RF ion systems produced commercially by Busek Inc. Busek produces three sizes of the radio frequency ion thrusters including a 1cm, 3cm and 7cm design. The 3 cm system fits the requirements for a CubeSat to the Moon mission or Lunar Cube as we designated the concept. Busek's RF ion thrusters utilize inductively-coupled plasma (ICP) discharge with xenon as propellant. Compatibility with other noble and condensable gases has been demonstrated. While maintaining the characteristic of high specific impulse of a typical DC ion thruster, utilizing the RF discharge eliminates the need for internal cathode and thus increases overall lifetime. Other advantages of RF discharge include fast start-up, precision thrust and rapid thrust response to RF power input. Without the use of internal cathode and permanent magnetic structure, the RF ion thrusters can be minimized for power and size, making them ideal for small satellite propulsion.

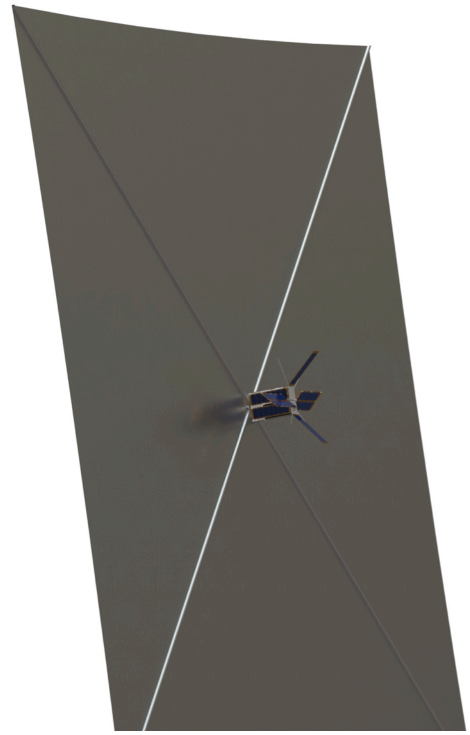

Figure 28: Lunar Flashlight. A concept for a Cubesat-based lunar mission to search for lunar water ice [Hayne et al., 2013b]. The spacecraft utilizes a navigable solar sail that also serves as a reflector to shine sunlight into permanently shadowed regions allowing detection with a multi-channel IR spectrometer. Courtesy JPL, NASA/MSFC, and Morehead State University.

An alternative low thrust propulsion technology holds great promise to enable small satellite-based exploration of the inner Solar System- navigable solar sails. Several precursor missions, including JAXA's IKAROS, NASA's Nanosail D, and The Planetary Society/Stellar Exploration's LightSail™-1 (the last built and tested, but not yet flown) have demonstrated the potential of the use of solar sail systems for propulsion, station-keeping, and inter-planetary navigation. Several commercial ventures are now capable of producing large, light-weight deployable sails that make interplanetary missions with small spacecraft viable.

These innovative propulsion systems will greatly enhance the capabilities of small satellites by allowing new orbital configurations, by allowing the creation of stable

[5] Paulo Lozano, the H.N. Slater Assistant Professor of Aeronautics and Astronautics at MIT

pointing platforms for Earth observing (i.e. nadir pointing) and astronomical observations, and by supporting lunar and beyond missions.

Radiation Tolerant Components

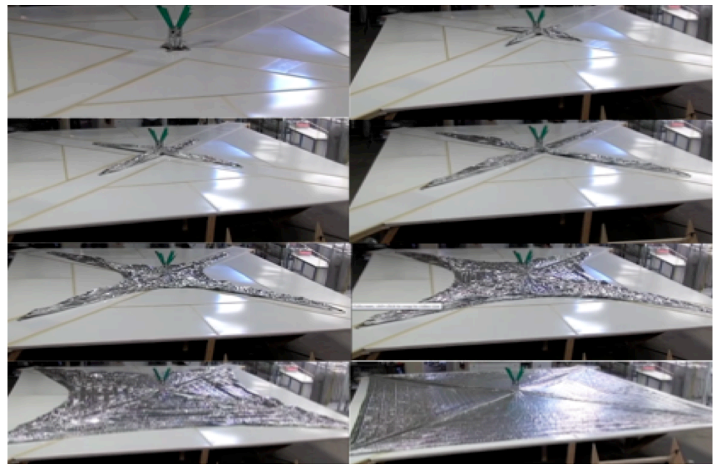

Figure 29: LightSail-1™ ground test deployment sequence at Stellar Exploration, requiring ~2 minutes. It deployed to 5.6 m on a side from ~1U volume. Using the same technology, Lunar Flashlight was proposed to carry a sail 8.7 m on a side deploying from 2U volume.

A significant challenge for any spacecraft venturing beyond Earth's magnetosphere is surviving both time-dependent buildup of damage by ionizing radiation (measured as total integrated dose – TID), and nearly instantaneous upsets and damage resulting from the passage of singular high energy charged particles (measured as linear energy transfer — LET). While all materials can be degraded by these phenomena, electronics are often the most sensitive. Low to moderate levels of TID are often accumulated by spacecraft in LEO, up to perhaps 10 krad [Si], and with much higher doses experienced over a spacecraft lifetime in satellites orbiting above 1000 km. Some beyond-Earth missions, including those to the Moon, can be accomplished experiencing similar doses to those successfully experienced by LEO CubeSats.

So-called Single Event Effects (SEE), of which single event upsets, single event latchups, and single event burnout are three progressively more severe categories, can be experienced by electronics in LEO, but such events are much more common far from Earth, where the magnetosphere does not deflect high energy cosmic rays that cause SEEs.

Electronic parts must be selected that are largely immune to both TID and LET up to levels appropriate to mission duration, location, and component criticality. Shielding can be used in some cases to lower TID, but no shielding that is practical for a small satellite can prevent SEEs. Clearly, space electronics have operated successfully beyond Earth for decades, but many of the COTS electronic components that enable inexpensive CubeSats are more susceptible to SEEs than "traditional" space-rated parts used on larger NASA and DOD missions. For components unlikely to experience single event burnout, electronics architecture, watchdog times, planned reboots, and multiple copies of memory can be effective in reducing system susceptibility to the effects of cosmic rays and so-called high-Z particles. The major space mission community, and increasingly the CubeSat community, keep and share records of electronic part reliability. It is also possible to determine ahead of time to some level of accuracy what will be the radiation susceptibility of parts of a particular design, and to test some parts in a manufacturing lot to predict the performance of other parts in the same lot, when it is possible to be sure that multiple parts were made more or less identically at the same time.

JPL's INSIRE mission is testing a variety of electronic parts in different applications and architectures aboard the spacecraft, for telecommunications, computing, power management, science instrument, and other functions. That short-duration mission (up to ~90 days) is expected to provide experience relevant subsequent beyond-Earth missions.

Attitude Determination and Control and Navigation Systems

A series of steady improvements in microcontroller technologies and attitude control sensors have led to small spacecraft achieving pointing accuracies to arc-minute and even arcsecond levels.The attitude control system (ACS) is a critical subsystem for any satellite mission since precise pointing is often required to meet mission objectives. The accuracy and precision requirements are extremely challenging for small satellites where limited volume, mass, and power are assignable to ACS. Most ACS systems utilized in small satellite systems incorporate fine control achieved through the use of three reaction wheels or three magnetorquers and one reaction wheel along the pitch axis. Attitude determination is generally achieved through the use of sun sensors, horizon sensors, star trackers, and inertial measurement units. Several COTS systems are available for microsats and nanosats including complete integrated ACS packages. These systems can achieve 10s of arcsecond accuracy (1- sigma) in pointing accuracy. Payload pointing precision at this level facilitates a wide variety of science missions with small spacecraft platforms.

Advanced Communications Systems

A new generation of spacecraft communications systems are now supporting high bandwidth, high throughput communications in small platforms with minimal power requirements. Frequency-agile software defined radios combined with innovative antenna systems (microstrip antenna arrays, inventive patch antennas, and reconfigurable antennas) hold the promise to push communications to higher and higher rates. Smallsat systems are currently achieving >10 Mb/s data downlink rates and have increased reliability and reduced power consumption. The use of directional antennas (made possible by improved attitude control) will allow the use of higher frequency downlinks. It has been shown that nanosatellites could achieve >100 Mb/s using a 1U Ka band transceiver.[6] These high throughput rates are essential systems enabling the use of smallsat platforms for lunar and planetary science missions.

Conclusions

Advances in electronics, electromechanical design miniaturized propulsion, precise ACS and energy storage have led to the possibility of developing low-cost, high performance small satellites in the 10kg to 100kg range that are capable of supporting interplanetary science research. Technologies are under development to support missions to Lunar Orbit and to the inner solar system utilizing these small, rapid development and cost-effective form factors. Meanwhile, contracting budgets for scientific research can no longer support numerous major satellite programs to lunar destinations and beyond. With the advent of micro and nanotechnologies and the evolution of these small, inexpensive satellite platforms, space exploration is primed for an evolutionary change.

[6] Nanosat Ka Band Communications- A Paradigm Shift in Small Satellite Data Throughput, Jan A. King, 26th Annual AILL/USU Conference on Small Satellites

5 Future Directions

5.1 Small Satellites as a Paradigm Shift in Planetary Science

With the recent success of large "flagship" planetary missions such as MSL and Cassini, the field of planetary science is currently at a zenith. However, as we look towards the future, diminished funding prospects compounded by increasing mission costs are raising significant concerns whether it will be possible to continue exploring our solar system at the pace we have become accustomed to.

Fortunately, small spacecraft technologies are becoming available that have the potential to enable significant reductions in the costs of planetary exploration. These smallsats (CubeSats, nanosats, etc.) promise to provide simple, flexible, modular spacecraft architectures that may be adapted for a range of scientific purposes. To date, the scientific and exploration capabilities of small spacecraft have been rather modest. Lacking capable propulsion, communications and instrument systems, and radiation-hardened parts, they are not currently in a position to compete with traditional planetary spacecraft. However, given general trends towards miniaturization and integration, it may be only a matter of time until it will be possible to build small spacecraft that can conduct groundbreaking science and exploration, providing more frequent and more diverse mission opportunities - especially for scientific problems where observations from multiple spacecraft is desirable. Small spacecraft could potentially supplant larger spacecraft when the ratio of science to cost becomes more favorable. This is mostly likely to occur first for nearby targets such as the moon and asteroids. Ultimately, low-mass small spacecraft could outperform "big" spacecraft on an absolute basis by providing faster travel times within the solar system and beyond, given the same total quantities of propulsive energy. The INSPIRE mission (sec. 2.2) will provide our first test of CubeSat technologies in interplanetary space, paving the way for future smallsat planetary missions.

5.2 Proposed Program for Lunar Ice Detection and Mapping

Access to lunar space and operations within lunar space remain key challenges to small satellite exploration and science at the Moon. To overcome these challenges we propose a multi-tier approach with the initial goal of proving the feasibility of lunar small satellites and final goal of creating a sustainable architecture of more capable instruments and spacecraft (Fig. 30).

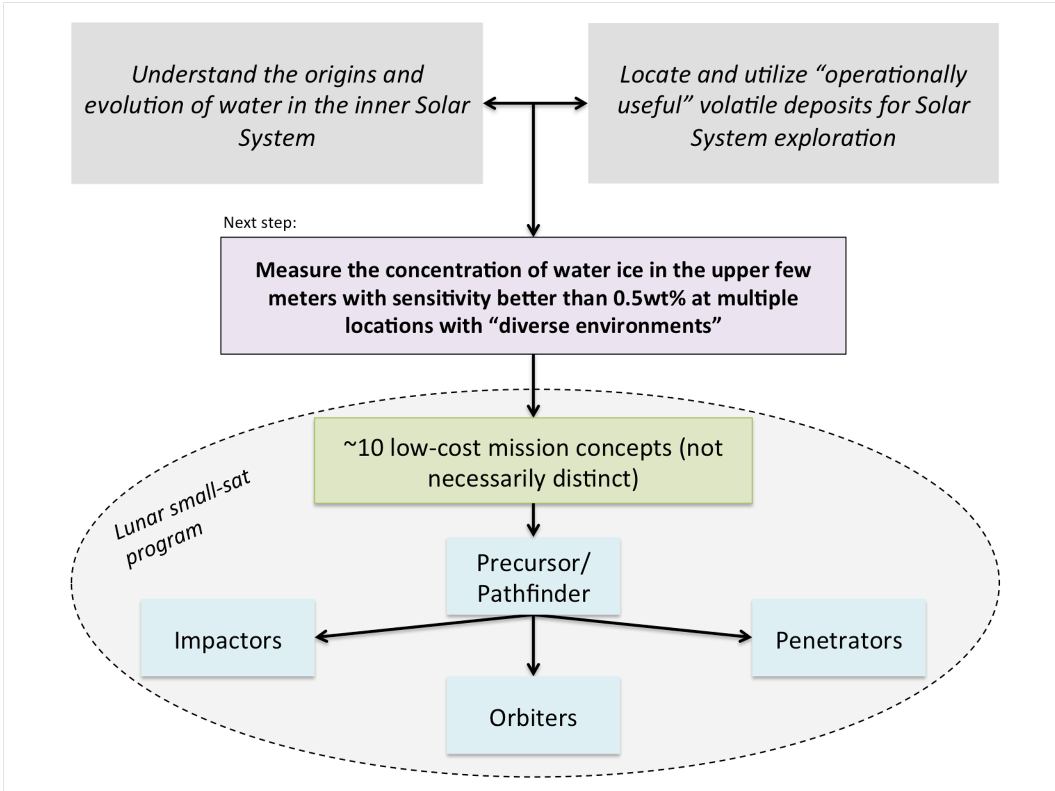

Figure 30: A framework for the proposed program of lunar exploration and science using small-sats. The two science and exploration goals feed directly into the key measurement objective, which would be accomplished by multiple small, low-cost missions.

First, we propose to send a precursor mission – a relatively simple nanosat mission (dubbed the Lunar Trailblazer, or LT) to the Moon. This mission would ideally fit within the 3U CubeSat form factor that has already been developed and tested in Earth orbit. The 6U CubeSat form factor would also be an option but would require a delay in implementation until 6U CubeSat launchers have been validated. The primary goals of the LT mission would be to demonstrate transfer orbit from a LEO, GEO, or Earth escape delivery (as these destinations are the likely to result in the most frequent "free rides"), and insertion into lunar orbit. The secondary goal is to demonstrate operations from lunar orbit, including attitude control and communications to Earth. The LT mission would consist of a relatively simple science payload, aimed at modest additional constraints in lunar ice distribution (e.g. low light camera, simple UV imager, simple thermal-infrared imager).

Following on the heels of a successful LT or series of LT missions, we propose to develop a sustainable architecture for accessing lunar space as a secondary payload on standard launch vehicles, allowing access to lunar study for orbiters, impactors, or penetrators. The goal of this architecture is to provide transport to lunar orbit

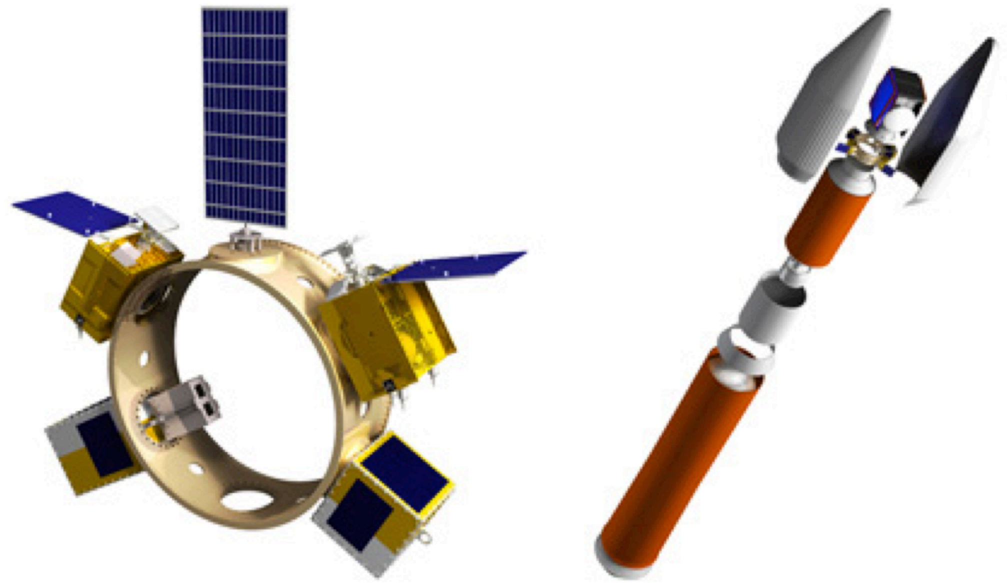

Figure 31: Evolved Expendable Launch Vehicle (EELV) Secondary Payload Adapter for the Atlas V launch vehicle. (Image credit: CSA Engineering)

and advanced communication capabilities within a larger spacecraft bus, which would go to lunar orbit with every launch, and to maximize the remaining volume available for nanosats and instrumentation. The ESPA ring, such as that used for the successful LCROSS mission, or similar structure would be an ideal candidate for this type of spacecraft (Fig. 30). Current estimates indicate that the ESPA ring could support up to six body mounted instruments with volumes ~9U or six independent 6U CubeSats and launchers or some combination therein. Additional space remains available within the center of the ESPA ring for fuel, power, and communications. The spacecraft bus could host instruments, deploy CubeSats, and provide communication relay for landed and orbital assets. Although the role of the spacecraft bus would depend on the specific mission that is developed, with every launch another bus would go to lunar orbit and expand the total capabilities of the system. A flexible architecture combined with the rapid development times associated with small satellites enables a unique capacity to test new technologies and adapt the program as new discoveries are made. With this program in place, a complete lunar water-ice exploration roadmap with a range of missions, including orbiter, impactors, and penetrators could be supported. Such mission architecture would be an ideal, relatively inexpensive, and modern method for addressing the critical science and engineering issues surrounding lunar water (Fig. 22).

5.3 Importance of University Involvement

Universities have teamed with government and industry to successfully explore space from the earliest days of the space program. Universities have provided key scientific and technical knowhow, research facilities and space hardware, as well as training grounds for the next generation's space explorers. In the United States, the universities' share in space research funding has steadily diminished over the years, but the key roles that universities play in the overall space exploration endeavor remain. The CubeSat form-factor was developed university professors and their students, and has rapidly emerged as the *de facto* standard for student-designed and built small-sats. In a future in which commodity commercial launch vehicles provide low-cost space access for miniaturized spacecraft, universities have the potential to assume an even greater role in the development of space missions and space technology.

Figure 31: Students at the University of Southern California assemble flight hardware for their first CubeSat. (Credit: USC)

6 Conclusions and Recommendations

This study comes at a key moment, at the juncture between a wave of tantalizing lunar polar data on the nature and abundance of lunar water, and the emergence of small spacecraft as potentially viable planetary explorers. Through the synthesis of published results and recent data, as well as technical discussions and analysis, the study participants came to the conclusion that many outstanding questions remain regarding lunar volatiles, and some of the more interesting of these could be addressed using small spacecraft. In this report and associated materials, we have identified several promising candidate mission and instrument concepts for fulfilling the proposed campaign of lunar exploration and science using small spacecraft. Based on these outcomes, the key recommendations of this study are:

1. An integrated statistical analysis of existing datasets should be performed, in order to address remaining ambiguities and quantify uncertainties regarding lunar volatiles
2. Active near-IR and passive thermal IR spectroscopy of ices, and microwave sounding of impact plumes are intriguing techniques that should be investigated through a focused technology development program
3. For near-future missions, the highest priority measurement for lunar volatiles should be to detect and map water ice at better than 0.5wt% in diverse thermal environments, in the upper few meters of regolith
4. A "Lunar Trailblazer" nano-satellite should be developed and launched within the next five years, with a scientific payload for investigating lunar volatiles
5. A program of rapid development and launch of small spacecraft to the Moon should be embarked upon, in order to advance the study of lunar volatiles, and prove small spacecraft technology for planetary science and exploration
6. Small spacecraft technologies should continue to be developed in collaboration with university partners, with enhanced student involvement where possible

While fulfilling these priorities will be an ambitious undertaking, we conclude that cost should not be prohibitive, as long as university involvement remains strong. Rather, addressing several key technical hurdles will allow this new avenue of Solar System exploration to unfold in the relatively near future.

References

A'Hearn, M. F., Belton, M. J. S., Delamere, W. A., Kissel, J., Klaasen, K. P., McFadden, L. A., ... & White, A. R. (2005), Deep impact: excavating comet Tempel 1, *Science*, *310*(5746), 258-264.

Allen, M., M. Delitsky, W. Huntress, Y. Yung, W.-H. Ip, R. Schwenn, H. Rosenbauer, E. Shelley, H. Balsiger, J. Geiss (1987), Evidence for methane and ammonia in the coma of Comet P/Halley, *Astron. Astrophys., 187*, 502–512.

Arnold, J. R. (1979), Ice in the lunar polar regions. *J. Geophys. Res., 84*, 5659-5668.

Basilevsky, A.T., A.M. Abdrakhimov, and V.A. Dorofeeva (2012), Water and other volatiles on the Moon: A review, *Solar System Research*, *46*, 99-118.

Becker, R. H., and Clayton, R. N. (1975) Nitrogen abundances and isotopic compositions in lunar samples. *Lunar Science Conference, 6th, Proceedings*. Volume 2. (A78-46668 21-91) 2, p. 2131-2149. New York, Pergamon Press, Inc., , Houston, TX.

Boardman, J. W., Pieters, C. M., Green, R. O., Lundeen, S. R., Varanasi, P., Nettles, J., ... & Taylor, L. A. (2011). Measuring moonlight: An overview of the spatial properties, lunar coverage, selenolocation, and related Level 1B products of the Moon Mineralogy Mapper. *J. Geophys. Res., 116*(E6).

Bodnarik, J. G., Burger, D. M., Burger, A., Evans, L. G., Parsons, A. M., Schweitzer, J. S., ... & Stassun, K. G. (2013), Time-resolved neutron/gamma-ray data acquisition for in situ subsurface planetary geochemistry, *Nuclear Instruments and Methods in Physics Research Section A: Accelerators, Spectrometers, Detectors and Associated Equipment*, *707*, 135-142.

Boyce, J. W., Liu, Y., Rossman, G. R., Guan, Y., Eiler, J. M., Stolper, E. M., & Taylor, L. A. (2010), Lunar apatite with terrestrial volatile abundances, *Nature*, *466* (7305), 466-469.

Brown, R. H. et al., Composition and Physical Properties of Enceladus' Surface, *Science, 311* (5766), 1425-1428.

Boynton, W. V., et al. (2004), "The Mars Odyssey gamma-ray spectrometer instrument suite." *2001 Mars Odyssey*. Springer Netherlands, 37-83.

Boynton, W.V., et al. High spatial resolution studies of epithermal neutron emission from the lunar poles: Constraints on hydrogen mobility, *J. Geophys. Res., 117*, E003979, 2012.

Bussey, D. B. J., & Spudis, P. D. (2000), Compositional studies of the Orientale, Humorum, Nectaris, and Crisium lunar basins, *J. Geophys. Res.*, *105* (E2), 4235-4243.

Calvin, W. M., L. H. Roach, F. P. Seelos, K. D. Seelos, R. O. Green, S. L. Murchie, and J. F. Mustard (2009), Compact Reconnaissance Imaging Spectrometer for Mars observations of northern Martian latitudes in summer, *J. Geophys. Res., 114*, E00D11, doi:10.1029/2009JE003348.

Campbell, D. B., Campbell, B. A., Carter, L. M., Margot, J. L., & Stacy, N. J. (2006), No evidence for thick deposits of ice at the lunar south pole, *Nature*, *443* (7113), 835-837.

Carvano, J. M., Migliorini, A., Barucci, A., Segura, M. (2006), Constraining the surface properties of Saturn's icy moons, using Cassini/CIRS emissivity spectra, *Icarus, 187*, 574-583.

Chabot, N.L. et al. Craters hosting radar-bright deposits in Mercury's north polar region: Areas of persistent shadow determined from MESSENGER images (2013), *J. Geophys. Res. 118*, 26-36.

Cheek, L. C., Pieters, C. M., Boardman, J. W., Clark, R. N., Combe, J. P., Head, J. W., ... & Taylor, L. A (2011), Goldschmidt crater and the Moon's north polar region: Results from the Moon Mineralogy Mapper (M3), *J. Geophys. Res., 116* (E6).

Clark, R. N. (2009), Detection of adsorbed water and hydroxyl on the Moon, *Science, 326*, 562-564.

Clark, R.N. and P.G. Lucey (1984), Spectral Properties of Ice-Particulate Mixtures and Implications for Remote Sensing I: Intimate Mixtures, *J. Geophys. Res., 89,* 6341-6348.

Cocks, F.H., P.A. Klenk, S.A. Watkins, W.N. Simmons, J.C. Cocks, E.E. Cocks, and J.C. Sussingham (2002), Lunar ice: adsorbed water on subsurface polar dust, *Icarus, 160*, 386.

Colaprete, A., et al. (2010), Detection of water in the LCROSS ejecta plume, *Science, 330*, 463-468.

Cook, J.C., et al. (2013), New upper limits on numerous atmospheric species in the native lunar atmosphere, *Icarus*, 681-687.

Cook, J. C., Stern, S. A., Feldman, P. D., Retherford, K. D., Gladstone, G. R., Greathouse, T. K., ... & Davis, M. W. (2014), Possible Detection of Argon in the Lunar Atmosphere as Seen by the LAMP Instrument on the Lunar Reconnaissance Orbiter, In *Lunar and Planetary Science Conference Abstracts* (Vol. 45, p. 2788).

Crider, D. and Killen, R. M. (2005), Burial rate of Mercury's polar volatile deposits, *Geophys. Res. Lett. 32*, L12201.

Crider, D. H., and R. R. Vondrak (2002), Hydrogen migration to the lunar poles by solar wind bombardment of the moon, *Adv. Space Res., 30*, 1869.

Crider, D.H., and R. R. Vondrak (2002), The solar wind as a possible source of lunar polar hydrogen deposits, *J. Geophys. Res., 105*, 26773.

Dyar, M.D., Hibbitts, C.A., Orlando, T.M. (2010), Mechanisms for incorporation of hydrogen in and on terrestrial planetary surfaces, *Icarus, 208*, 425-437.

Emery JP et al. (2005), Near-infrared (0.8–4.0 μm) spectroscopy of Mimas, Enceladus, Tethys, and Rhea, *Astron. & Astrophys.*, *435*, 353-362.

Fa, W., & Jin, Y. Q. (2010), A primary analysis of microwave brightness temperature of lunar surface from Chang-E 1 multi-channel radiometer observation and inversion of regolith layer thickness. *Icarus*, *207* (2), 605-615.

Feldman, W.C., S. Maurice, B.L. Barraclough A.B. Binder, R.C. Elphic, and D.J. Lawrence (1998), Fluxes of fast and epithermal neutrons from lunar prospector: Evidence for water ice at the lunar poles, *Science, 281*, 1496-1500.

Feldman, W.C., D.J. Lawrence, R.C. Elphic, B.L. Barraclough, S. Maurice, I. Genetay, and A.B. Binder (2000), Polar hydrogen deposits on the Moon, *J. Geophys. Res., 105*, 4175-4196.

Feldman, W.C. et al. (2001), Evidence for water ice near the lunar poles, *J. Geophys. Res., 106*, 23231-23251.

Gibson Jr, E. K., & Moore, G. W. (1973), Volatile-rich lunar soil: evidence of possible cometary impact. *Science*, *179* (4068), 69-71.

Goddard R., in *The Papers of Robert H. Goddard*, ed. by E. C. Goddard, G. E. Pendray (McGraw-Hill, New York, 1920), pp. 413–430.

Gladstone, G.R., et al. Far-ultraviolet reflectance properties of the Moon's permanently shadowed regions (2010), *J. Geophys. Res*., *117*, E00H04.

Gladstone, G. R., Retherford, K. D., Egan, A. F., Kaufmann, D. E., Miles, P. F., Parker, J. W., ... & Stern, S. A. (2012), Far-ultraviolet reflectance properties of the Moon's permanently shadowed regions, *J. Geophys. Res., 117* (E1).

Green, R. O., Pieters, C., Mouroulis, P., Eastwood, M., Boardman, J., Glavich, T., ... & Tseng, H. (2011), The Moon Mineralogy Mapper (M3) imaging spectrometer for lunar science: Instrument description, calibration, on-orbit measurements, science data calibration and on-orbit validation, *J. Geophys. Res.*, *116* (E10).

Groussin, O., A'Hearn, M. F., Li, J. Y., Thomas, P. C., Sunshine, J. M., Lisse, C. M., ... & Delamere, W. A. (2007), Surface temperature of the nucleus of Comet 9P/Tempel 1, *Icarus*, *191*(2), 63-72.

Gulkis, S., Frerking, M., Crovisier, J., Beaudin, G., Hartogh, P., Encrenaz, P., ... & Spilker, T. (2007), MIRO: microwave instrument for Rosetta Orbiter, *Space Sci. Rev.*, *128* (1-4), 561-597.

Gulkis, S., Keihm, S., Kamp, L., Lee, S., Hartogh, P., Crovisier, J., ... & Mann, I. (2012), Continuum and spectroscopic observations of asteroid (21) Lutetia at millimeter and submillimeter wavelengths with the MIRO instrument on the Rosetta spacecraft, *Planet. and Space Sci.*, *66* (1), 31-42.

Hampton, D. L., Baer, J. W., Huisjen, M. A., Varner, C. C., Delamere, A., Wellnitz, D. D., ... & Klaasen, K. P. (2005), An overview of the instrument suite for the Deep Impact mission, *Space Science Reviews*, *117* (1-2), 43-93.

Hansen, G. B. (2009), Calculation of single-scattering albedos: Comparison of Mie results with Hapke approximations, *Icarus*, *203* (2), 672-676.

Hansen, G. B., and T. B. McCord (2008), Widespread CO2 and other non-ice compounds on the anti-Jovian and trailing sides of Europa from Galileo/NIMS observations, *Geophys. Res. Lett., 35*, L01202, doi:10.1029/2007GL031748.

Hapke, B. (1993), *Theory of Reflectance and Emittance Spectroscopy*, Cambridge Univ. Press, Cambridge, UK.

Hayne, P.O., et al. (2013a), Small scale cold traps on airless planetary bodies, *Bull. Am. Astron. Soc.,* #107.03.

Hayne, P. O., Cohen, B. A., Sellar, R. G., Staehle, R., Toomarian, N., & Paige, D. A. (2013b), Lunar Flashlight: Mapping Lunar Surface Volatiles Using a Cubesat. *LPI Contributions*, *1748*, 7045.

Hendrix, A. R., et al. (2012), The lunar far-UV albedo: Indicator of hydration and weathering, *J. Geophys. Res.*, *117*, E12001.

Hermalyn, B., Schultz, P. H., & Colaprete, A. (2009), LCROSS impact conditions and ejecta evolution: Insight from experiments, In *AGU Fall Meeting Abstracts* (Vol. 1, p. 0034).

Hibbitts, C.A., G. Grieves, M.J. Poston, M.D. Dyar, A.B. Alexandrov, M.A. Johnson, and T.M. Orlando (2011), Thermal stability of water and hydroxyl on the surface of the Moon from temperature-programmed desorption measurements of lunar analog materials, *Icarus, 213*, 64-72.

Hodges, R. R. (2002), Ice in the lunar polar regions revisited, *J. Geophys. Res.*, *107*, 5011.

Howett, C. J. A., Spencer, J. R., Pearl, J., Segura, M. (2010), Thermal inertia and bolometric Bond albedo values for Mimas, Enceladus, Tethys, Dione, Rhea and Iapetus as derived from Cassini/CIRS measurements, *Icarus, 206* (2), 573-593.

Hudson, R. L., Moore, M. H., Ferrante, R. F., Gerakines, P. A., & Loeffler, M. J. (2013), IR Measurements of Icy Solids of the Outer Solar System: A New Spectral Database. In *AAS/Division for Planetary Sciences Meeting Abstracts* (Vol. 45).

Jiménez, C., Gulkis, S., Beaudin, G., Encrenaz, T., Eriksson, P., Kamp, L., ... & Buehler, S. A. (2013), Sub-millimeter observations of the terrestrial atmosphere during an Earth flyby of the MIRO sounder on the Rosetta spacecraft, *Planet. and Space Sci.*, *82*, 99-112.

Keihm, S. J. (1984), Interpretation of the lunar microwave brightness temperature spectrum: Feasibility of orbital heat flow mapping, *Icarus*, *60* (3), 568-589

Killen, M.M. and Ip, W-H. The surface-bounded atmospheres of Mercury and the Moon. Rev. Geophys., 37:361-406, 2010.

Klesh, A. T., J. C. Castillo-Rogez (2012), Applications of NanoSats to Planetary Exploration, *AIAA SPACE 2012 Conf.*, abstract no. 2012-5326.

Klima, R., Cahill, J., Hagerty, J., & Lawrence, D. (2013). Remote detection of magmatic water in Bullialdus Crater on the Moon. *Nature Geoscience*, *6*, 737-741.

Langevin, Y., F. Poulet, J. P. Bibring, and B. Gondet (2005), Summer evolution of the north polar cap of Mars as observed by OMEGA/Mars express, *Science, 307* (5715), 1581–1584, doi:10.1126/science.1109438.

Langevin, Y., J.-P. Bibring, F. Montmessin, F. Forget, M. Vincendon, S. Doute´, F. Poulet, and B. Gondet (2007), Observations of the south seasonal cap of Mars during recession in 2004–2006 by the OMEGA visible/near-infrared imaging spectrometer on board Mars Express, *J. Geophys. Res., 112*, E08S12, doi:10.1029/2006JE002841.

Lawrence, D.J. et al. (2013), Evidence of water ice near Mercury's pole from MESSENGER neutron spectrometer measurements, *Science, 339*, 292-296.

Litvak, M. L., Mitrofanov, I. G., Barmakov, Y. N., Behar, A., Bitulev, A., Bobrovnitsky, Y., ... & Vostrukhin, A. (2008), The dynamic albedo of neutrons (DAN) experiment for NASA's 2009 Mars Science Laboratory, *Astrobiology*, *8*(3), 605-612.

Litvak, M. L., Mitrofanov, I. G., Sanin, A., Malakhov, A., Boynton, W. V., Chin, G., ... & Zuber, M. T. (2012), Global maps of lunar neutron fluxes from the LEND instrument, *J. Geophys. Res.*, *117* (E12).

Liu, Y., Spicuzza, M.J., Craddock, P.R., Day, J.M.D., Valley, J.W., Dauphas, N., and Taylor, L.A. (2010), Oxygen and iron isotope constraints on near-surface fractionation effects and the composition of lunar mare basalt source regions, *Geochimica Et Cosmochimica Acta*, *74* (21), 6249-6262.

Liu, Y., Guan, Y., Zhang, Y., Rossman, G. R., Eiler, J. M., & Taylor, L. A. (2012), Direct measurement of hydroxyl in the lunar regolith and the origin of lunar surface water, *Nature Geoscience*, *5* (11), 779-782.

Livengood, T. A., G. Chin, R. Z. Sagdeev, I. G. Mitrofanov, W. V. Boynton, L. G. Evans, M. L. Litvak, T. P. McClanahan, A. B. Sanin, R. D. Starr (2014) Evidence for Diurnally Varying Hydration at the Moon's Equator from the Lunar Exploration Neutron Detector (LEND), *45th Lunar and Planetary Science Conference*, #1777, p.1507.

Lorenz, R. D. (2011), Planetary penetrators: Their origins, history and future, *Advances in Space Research*, *48*(3), 403-431.

Lucey, P. G. (2009a), The poles of the Moon, *Elements, 5,* 41-46.

Lucey, P. G. (2009b), A lunar waterworld, *Science, 326*, 531-532.

Lucey, P. G., Neumann, G. A., Paige, D. A., Riner, M. A., Mazarico, E. M., Smith, D. E., ... & Song, E. (2014, March). Evidence for Water Ice and Temperature Dependent Space Weathering at the Lunar Poles from Lola and Diviner. In *Lunar and Planetary Science Conference Abstracts* (Vol. 45, p. 2325).

Maldoni, M. M., Smith, R. G., Robinson, G., Rookyard, V. L., 1998. A study of the 2.5-25 um of H2O ice. Mon. Not. R. Astron. Soc., 298, 1, 251-258.

Marty, B., Chaussidon, M., Wiens, R.C., Jurewicz, A.J.G., and Burnett, D.S. (2011), A 15N-Poor Isotopic Composition for the Solar System As Shown by Genesis Solar Wind Samples, *Science, 332* (6037), 1533-1536.

Marty, B. (2012) The origins and concentrations of water, carbon, nitrogen and noble gases on Earth. *Earth and Planetary Science Letters*, 313–314(0), 56-66.

Maurice, S., Lawrence, D. J., Feldman, W. C., Elphic, R. C., & Gasnault, O. (2004), Reduction of neutron data from Lunar Prospector, *J. Geophys. Res.*, *109*(E7).

McCord, T.B., et al. Sources and physical processes responsible for OH/H2O in the lunar soil as revealed by the Moon Mineralogy Mapper (M3). J. Geophys. Res., 116, E00G05, 2011.

McKinney, G. W., Lawrence, D. J., Prettyman, T. H., Elphic, R. C., Feldman, W. C., & Hagerty, J. J. (2006), MCNPX benchmark for cosmic ray interactions with the Moon, *J. Geophys. Res., 111*(E6).

McKeegan, K.D., Kallio, A.P.A., Heber, V.S., Jarzebinski, G., Mao, P.H., Coath, C.D., Kunihiro, T., Wiens, R.C., Nordholt, J.E., Moses, R.W., Reisenfeld, D.B., Jurewicz, A.J.G., and Burnett, D.S. (2011), The Oxygen Isotopic Composition of the Sun Inferred from Captured Solar Wind, *Science, 332* (6037), 1528-1532.

Mitrofanov, I.G., et al. (2010), Hydrogen mapping of the lunar south pole using the LRO neutron detector experiment LEND, *Science, 330*, 483-486.

Mitrofanov, I.G., et al. (2012), Testing polar spots of water-rich permafrost on the moon: LEND observations onboard LRO*, J. Geophys. Res.*, *117*, E00H27.

Moore, M. H., Hudson, R. L. (1992), Far-Infrared Spectral Studies of Phase Changes in Water Ice Induced by Proton Irradiation, *Astrophys. J.,* 401, 353-360.

Morgan, T. H., & Shemansky, D. E. (1991), Limits to the lunar atmosphere, *J. Geophys. Res.*, *96*(A2), 1351-1367.

Mosher, T. J., & Lucey, P. (2006), Polar Night: A lunar volatiles Expedition, *Acta Astronautica*, *59*(8), 585-592.

Mustard, J.F., M. Adler, A. Allwood, D.S. Bass, D.W. Beaty, J.F. Bell III, W.B. Brinckerhoff, M. Carr, D.J. Des Marais, B. Drake, K.S. Edgett, J. Eigenbrode, L.T. Elkins-Tanton, J.A. Grant, S. M. Milkovich, D. Ming, C. Moore, S. Murchie, T.C. Onstott, S.W. Ruff, M.A. Sephton, A. Steele, A. Treiman (2013), "Report of the Mars 2020 Science Definition Team", 154 pp., posted July, 2013, by the Mars Exploration Program Analysis Group (MEPAG) at http://mepag.jpl.nasa.gov/reports/MEP/Mars_2020_SDT_Report_Final.pdf.

Neumann, G. A., Cavanaugh, J. F., Sun, X., Mazarico, E. M., Smith, D. E., Zuber, M. T., ... & Barnouin, O. S. (2013), Bright and dark polar deposits on Mercury: Evidence for surface volatiles, *Science*, *339*(6117), 296-300.

Normile, D., & Bagla, P. (2007), Asian Powers Shoot for the Moon With Orbiting Research Missions, *Science*, *317*(5842), 1163-1163.

Nozette, S., C.L. Lichtenberg, P.D. Spudis, R. Bonner, W. Ort, E. Malaret, M. Robinson, and E.M. Shoemaker (1996), The Clementine bistatic radar experiment, *Science, 274*, 1495-1498.

Nozette, S., Spudis, P., Bussey, B., Jensen, R., Raney, K., Winters, H., ... & Robinson, M. (2010), The Lunar Reconnaissance Orbiter miniature radio frequency (Mini-RF) technology demonstration, *Space Sci. Rev.*, *150*(1-4), 285-302.

Ootsubo, T., Sugita, S., Kadono, T., Honda, M., Sakon, I., Kawakita, H., Watanabe, J. (2009), Mid-Infrared Observations of the Dust Plume from Comet 9P/Tempel 1 Generated by the Deep Impact Collision Using Subaru/COMICS, *Workshop on Dust in Planetary Systems*, ESA SP-643, 45-49.

Ostro, S. J., Campbell, D. B., Pettengill, G. H., & Shapiro, I. I. (1980), Radar observations of the icy Galilean satellites, *Icarus*, *44*(2), 431-440.

Paige, D. A., Foote, M. C., Greenhagen, B. T., Schofield, J. T., Calcutt, S., Vasavada, A. R., Preston, D. J., Taylor, F. W., Allen, C. C., Snook, K. J., Jakosky, B. M., Murray, B. C., Soderblom, L. A., Jau, B., Loring, S., Bulharowski, J., Bowles, N. E., Thomas, I. R., Sullivan, M. T., Avis, C., de Jong, E. M., Hartford, W., McCleese, D. J., 2009. The Lunar Reconnaissance Orbiter Diviner Lunar Radiometer Experiment. Space Sci. Rev., 150, 1-4, 125-160.

Paige, D. A., Siegler, M. A., Zhang, J. A., Hayne, P. O., Foote, E. J., Bennett, K. A., ... & Lucey, P. G. (2010). Diviner lunar radiometer observations of cold traps in the Moon's south polar region. *Science*, *330*(6003), 479-482.

Parsons, A., Bodnarik, J., Evans, L., Floyd, S., Lim, L., McClanahan, T., ... & Trombka, J. (2011), Active neutron and gamma-ray instrumentation for in situ planetary science applications, *Nuclear Instruments and Methods in Physics Research Section A: Accelerators, Spectrometers, Detectors and Associated Equipment*, *652*(1), 674-679.

Pearl, J. C., Smith, M. D., Conrath, B. J., Bandfield, J. L., & Christensen, P. R. (2001), Observations of martian ice clouds by the Mars Global Surveyor Thermal Emission Spectrometer: The first martian year, *J. Geophys. Res., 106*(E6), 12325-12338.

Paige, D.A. et al. (2013), Thermal stability of volatiles in the north polar region of Mercury, *Science, 339*, 300-303.

Patterson, G. W., Bussey, D. B. J., Stickle, A. M., Cahill, J. T. S., Carter, L. M., & Team, M. R. (2014), Mini-RF and the Curious Case of Cabeus Crater, In *Lunar and Planetary Science Conference Abstracts* (Vol. 45, p. 2765).

Pieters, C.M., et al. Character and spatial distribution of OH/H2O on the surface of the Moon seen by M3 on Chandrayaan-1. Science, 326:568-572, 2009.

Pilorget, C., Vincendon, M., & Poulet, F. (2013). A radiative transfer model to simulate light scattering in a compact granular medium using a Monte–Carlo approach: Validation and first applications. *J. Geophys. Res.*, *118*(12), 2488-2501.

Poston, M.J., et al. (2013), Water interactions with micronized lunar surrogates JSC-1A and albite under ultra-high vacuum with application to lunar observations, *J. Geophys. Res., 118*, 105-115.

Potter, A. E., & Del Duca, B. (1964), Lifetime in space of possible parent molecules of cometary radicals, *Icarus*, *3*(2), 103-108.

Raney, R. K., Spudis, P. D., Bussey, B., Crusan, J., Jensen, J. R., Marinelli, W., ... & Winters, H. (2011), The lunar Mini-RF Radars: Hybrid polarimetric architecture and initial results, In *Proceedings of the IEEE*, *99*(5), 808-823.

Rink, C., "NASA Picks Small Spacecraft Propulsion Systems for Development," Release 13-029, July 11, 2013 http://www.nasa.gov/larc/nasa-picks-small-spacecraft-propulsion-systems-for-development/#.UtcWnPYXiK4

Saal, A. E., Hauri, E. H., Cascio, M. L., Van Orman, J. A., Rutherford, M. C., & Cooper, R. F. (2008), Volatile content of lunar volcanic glasses and the presence of water in the Moon's interior, *Nature*, *454*(7201), 192-195.

Saal, A. E., Hauri, E. H., Van Orman, J. A., and Rutherford, M. J. (2013), Hydrogen Isotopes in Lunar Volcanic Glasses and Melt Inclusions Reveal a Carbonaceous Chondrite Heritage, *Science*, *340*, 1317-1320.

Sanders, G (2013), Future Missions & In Situ Resource Utilization (ISRU) Requirements, http://www.kiss.caltech.edu/workshops/lunarFice2013/presentations/sanders.pdf

Sanin, A. B., Mitrofanov, I. G., Litvak, M. L., Boynton, W. V., Chin, G., Evans, L. G., ... & Starr, R. D. (2014), Estimation of Hydrogen Concentration in Lunar South Polar Regions. In *Lunar and Planetary Science Conference Abstracts* (Vol. 45, p. 1358).

Schorghofer, N. (2007), Theory of ground ice stability in sublimation environments, *Phys. Rev. E*, *75*(4), 041201.

Schorghofer, N. (2008), The lifetime of ice on main belt asteroids, *Astrophys. J.*, *682*(1), 697.

Schorghofer, N (2012), On the theory of migration of water on the Moon, *Lunar & Planet. Sci. Conf., 43*, abstract #1110.

Schorghofer, N. and O. Aharonson (2014), The lunar thermal ice pump, *Submitted*, 2013.

Schultz, P. H. (2006), Shooting the Moon: Constraints on LCROSS targeting, *LPI Contributions*, *1327*, 14-15.

Schultz, P. H., Eberhardy, C. A., Ernst, C. M., A'Hearn, M. F., Sunshine, J. M., & Lisse, C. M. (2007), The Deep Impact oblique impact cratering experiment, *Icarus*, *191*(2), 84-122.

Schultz, P. H., Hermalyn, B., Colaprete, A., Ennico, K., Shirley, M., & Marshall, W. S. (2010), The LCROSS cratering experiment. *Science*, *330*(6003), 468-472.

Siegler, M., Aharonson, O., Carey, E., Choukroun, M., Hudson, T., Schorghofer, N., & Xu, S. (2012), Measurements of thermal properties of icy Mars regolith analogs, *J. Geophys. Res. , 117*(E3).

Slade, M.A., B. J. Butler, D.O. Muhleman (1992), Mercury radar imaging - evidence for polar ice. *Science, 258*, 635-640.

Smith, M. D., Pearl, J. C., Conrath, B. J., Christensen, P. R., 2001. Thermal Emission Spectrometer results: Mars atmospheric thermal structure and aerosol distribution. J. Geophys. Res., 106, 23929-23945.

Smrekar, S., Catling, D., Lorenz, R., Magalhães, J., Moersch, J., Morgan, P., ... & Blaney, D. (1999), Deep Space 2: the Mars microprobe mission, *J. Geophys. Res.*, *104*(E11), 27013-27030.

Spicuzza, M.J., Day, J.M.D., Taylor, L.A., and Valley, J.W. (2007), Oxygen isotope constraints on the origin and differentiation of the Moon, *Earth and Planetary Science Letters*, 253(1-2), 254-265.

Spudis, P. D., Bussey, D. B. J., Baloga, S. M., Butler, B. J., Carl, D., Carter, L. M., ... & Winters, H. L. (2010), Initial results for the north pole of the Moon from Mini-SAR, Chandrayaan-1 mission, *Geophysical Research Letters*, *37*(6).

Spudis, P.D., et al. (2013), Evidence for water ice on the moon: Results for anomalous polar craters from the LRO Mini-RF imaging radar, *J. Geophys. Res., 118*, 2016-2029.

Sridharan, R., et al. 'Direct' evidence for water (H2O) in the sunlit lunar ambience from CHACE on MIP of Chandrayaan I. Planetary & Space Science, 58:947-950, 2010.

Stacy, N.J.S., D.B. Campbell, and P.G. Ford (1997), Arecibo radar mapping of the lunar poles: A search for ice deposits, *Science, 276*, 1527.

Staehle, R. L., D. Blaney, H. Hemmati, D. Jones, A. Klesh, P. Liewer, J. Lazio, M. Wen-Yu Lo, P. Mouroulis, N. Murphy, P. J. Pingree, T. Wilson, B. Anderson, C. C. Chow II, B. Betts, L. Friedman, J. Puig-Suari, A. Williams, and T. Svitek (2013), "Interplanetary CubeSats: Opening the Solar System to a Broad Community at Lower Cost", *Journal of Small Satellites (JoSS), Vol. 2*, No. 1, pp. 161-186.

Starr, R. D., Evans, L. G., Parsons, A. M., Trombka, J. I., Groves, J., Akkurt, H., ... & Schweitzer, J. (2007), Combined Gamma-Ray Spectrometer and Pulsed Neutron Generator System for In-Situ Planetary Geochemical Analysis, In *Lunar and Planetary Institute Science Conference Abstracts* (Vol. 38, p. 1919).

Starukhina, L.V. (2001), Water detection on atmosphereless celestial bodies: Alternative explanations of the observations*, J. Geophys. Res., 106*, 14701-14710.

Starukhina, L.V. (2006), Polar regions of the moon as a potential repository of solar-wind-implanted gases, *Adv. Space Res.*, *37*, 50-58.

Stern, S.A (1999), The lunar atmosphere: history, status, current problems, and context*, Rev. Geophys., 37*, 453-491.

Stern, S. A., Retherford, K. D., Tsang, C. C. C., Feldman, P. D., Pryor, W., & Gladstone, G. R. (2012), Lunar atmospheric helium detections by the LAMP UV spectrograph on the Lunar Reconnaissance Orbiter, *Geophys. Res. Lett.*, *39*(12).

Sunshine, J.M. et al. Temporal and spatial variability of lunar hydration as observed by the Deep Impact Spacecraft. Science, 326:565-568, 2009.

Thomson, B. J., et al. (2012), An upper limit for ice in Shackleton crater as revealed by LRO Mini-RF orbital radar, *Geophys. Res. Lett., 39*, L14201.

Trombka, J. I., Starr, R. D., Groves, J., Akkurt, H., Evans, L. G., McCoy, T. J., ... & McClanahan, T. P. (2005). A pulsed neutron gamma-ray system for Mars rover missions, In *Aerospace Conference, 2005 IEEE* (pp. 681-690).

Vasavada, A. R., Paige, D. A., & Wood, S. E. (1999), Near-surface temperatures on Mercury and the Moon and the stability of polar ice deposits, *Icarus*, *141*(2), 179-193.

Ward, W. R. (1975), Past orientation of the lunar spin axis*, Science 189, 377-379*.

Warren, S. G. (1984), Optical constants of ice from the ultraviolet to the microwave. *Applied Optics*, *23*(8), 1206-1225.
Watson, K., B.C. Murray, H. Brown (1961a), On the possible presence of ice on the Moon, *J. Geophys. Res.*, *66*, 1598.
Watson, K., B.C. Murray, H. Brown (1961b), The behavior of volatiles on the lunar surface, *J. Geophys. Res.*, *66*, 3033.
Wieler, R., Pedroni, A., and Leya, I. (2000), Cosmogenic neon in mineral separates from Kapoeta: No evidence for an irradiation of its parent body regolith by an early active Sun, *Meteoritics & Planetary Science*, 35(2), 251-257.
Yung, Y. L. and Dissley, R. W. (1992), Deuterium in the Solar System, In: "Isotope Effects in Gas-Phase Chemistry", ACS Symposium Series Vol 502, 369-389.
Zhang, J.A., and D.A. Paige. Cold-trapped organic compounds at the poles of the Moon and Mercury: Implications for origins. Geophys. Res. Lett., 36, L16203, 2009.
Zuber, M. T., Head, J. W., Smith, D. E., Neumann, G. A., Mazarico, E., Torrence, M. H., ... & Melosh, H. J. (2012), Constraints on the volatile distribution within Shackleton crater at the lunar south pole, *Nature*, *486*(7403), 378-381.

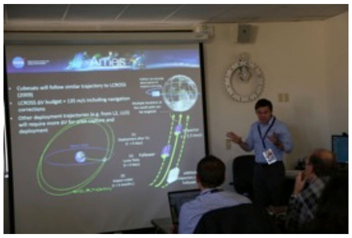
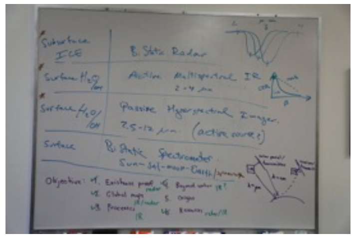






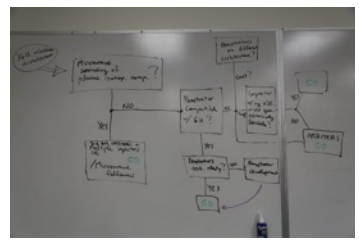

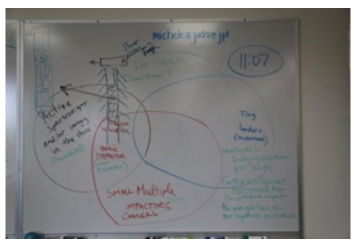



Keck

KISS - SAT